Published in final edited form as:
J Neurochem. 2014 May ; 129(3): 400–412. doi:10.1111/jnc.12617.

Fatty acid biosynthesis from glutamate and glutamine is specifically induced in neuronal cells under hypoxia

Stephen A. Brose, **Amanda L. Marquardt**, and **Mikhail Y. Golovko***
Department of Pharmacology, Physiology, and Therapeutics, University of North Dakota, Grand Forks, ND 58202-9037

Abstract

Hypoxia is involved in many neuronal and non-neuronal diseases, and defining the mechanisms for tissue adaptation to hypoxia is critical for the understanding and treatment of these diseases. One mechanism for tissue adaptation to hypoxia is increased glutamine and/or glutamate (Gln/Glu) utilization. To address this mechanism, we determined total Gln/Glu incorporation into lipids and fatty acids in both primary neurons and a neuronal cell line under normoxic and hypoxic conditions and compared this to non-neuronal primary cells and non-neuronal cell lines. Incorporation of Gln/Glu into total lipids was dramatically and specifically increased under hypoxia in neuronal cells including both primary (2.0- and 3.0- fold for Gln and Glu, respectively) and immortalized cultures (3.5- and 8.0- fold for Gln and Glu, respectively), and 90% to 97% of this increase was accounted for by incorporation into fatty acids (FA) depending upon substrate and cell type. All other non-neuronal cells tested demonstrated decreased or unchanged FA synthesis from Gln/Glu under hypoxia. Consistent with these data, total FA mass was also increased in neuronal cells under hypoxia that was mainly accounted for by the increase in saturated and monounsaturated FA with carbon length from 14 to 24. Incorporation of FA synthesized from Gln/Glu was increased in all major lipid classes including cholesteryl esters, TAGs, DAGs, free FA, and phospholipids, with the highest rate of incorporation into TAGs. These results indicate that increased FA biosynthesis from Gln/Glu followed by esterification may be a neuronal specific pathway for adaptation to hypoxia.

Keywords

lipids; fatty acids; fatty acid biosynthesis; hypoxia; glutamate; glutamine

INTRODUCTION

Hypoxia is an important pathological condition of many neurological and non-neurological diseases, including stroke, head trauma, brain injury, tumor development, toxicosis, heart disease, vascular inflammation, atherosclerotic and ischemic vascular disease, aging, and neurodegenerative diseases (Gallagher & Hackett 2004, Wilson *et al.* 2009, Lin *et al.* 2013,

*Corresponding author: Mikhail Y. Golovko, Department of Pharmacology, Physiology, and Therapeutics, School of Medicine and Health Sciences, University of North Dakota, 501 N. Columbia Rd., Grand Forks, ND 58202-9037, mikhail.golovko@med.und.edu, 701-777-2305 phone, 701-777-4490 fax.

The authors have no conflict of interest to declare.

Raymond *et al.* 2011, Clambey *et al.* 2012, Kirby *et al.* 2012). Functional and behavioral deficits associated with nervous system damage from hypoxia are associated with neuronal damage in the hippocampus and cortex (Hartman *et al.* 2005, Maiti *et al.* 2007, Hota *et al.* 2008). The tissue adapts to these conditions through activation of anaerobic metabolism in order to protect the nervous system from further damage. Thus, defining molecular mechanisms for tissue adaptation to hypoxic conditions is critical for the understanding and pharmacological treatment of many pathophysiological processes in the nervous system where hypoxia is involved.

One of the mechanisms for tissue, including brain and tumor, adaptation to anaerobic conditions is increased glutamine and/or glutamate (Gln/Glu) consumption (Chen & Russo 2012, Pascual *et al.* 1998, DeBerardinis *et al.* 2007, Schippers *et al.* 2012) at levels exceeding that required for protein biosynthesis (DeBerardinis et al. 2007). In addition, the relative contribution of Gln/Glu utilization for lipogenic acetyl-CoA through reductive carboxylation of α-ketoglutarate is increased under hypoxia in all cell types tested (Leonardi *et al.* 2012, Metallo *et al.* 2012, Gameiro *et al.* 2013), indicating that lipid synthesis from Gln/Glu might be increased under hypoxia. Although the relative contribution of Gln *versus* glucose for lipogenic acetyl-CoA synthesis is increased under hypoxia (Leonardi et al. 2012, Metallo et al. 2012, Gameiro et al. 2013), to the best of our knowledge, the absolute incorporation of Gln/Glu into lipids and fatty acids (FA) under hypoxic conditions in neuronal cells has not been previously determined.

In the present study, we determined the incorporation of Gln/Glu into lipids and FA in a neuronal cell line and primary neurons under hypoxic conditions, and compared the results to non-neuronal cell lines and primary cell cultures. The total incorporation of Gln/Glu into total lipids was dramatically and specifically increased in neuronal cells, while it was decreased or unchanged in all non-neuronal cells tested. Incorporation into total (esterified and free) FA accounted for 90% to 97% of the substrate incorporation into neuronal lipids depending upon substrate and cell type. These results indicate that FA biosynthesis from Gln/Glu might be a specific adaptation pathway for neuronal cells under hypoxia.

MATERIALS AND METHODS

Materials

SH-SY5Y and BV2 cell lines were a gift from Dr. Colin Combs. All other cell lines were purchased from the American Type Culture Collection (ATCC, Manassas, VA). E-18 primary rat cortical neurons, E-19 primary rat astrocytes, horse serum, Dulbecco's Modified Eagle Medium/F-12 (DMEM/F-12), Minimum Essential Medium (MEM) with and without L-glutamine and Neurobasal media were purchased from Life Technologies (Grand Island, NY). Fetal Bovine Serum (FBS) was purchased from Serum Source International (Charlotte, NC). L-[U-^{14}C] glutamine (Gln, 275 mCi/mmol), L-[U-^{14}C] glutamic acid (Glu, 260 mCi/mmol), D-[U-^{14}C] glucose (Glc, 289 mCi/mmol), L-[U- ^{14}C] aspartic acid (Asp, 200 mCi/mmol) and [1,^{14}C] glycerol trioleate (50 mCi/mmol) were purchased from PerkinElmer (Waltham, MA). Throughout the text, the fatty acids are represented by "number of carbons : number of double bonds", and where this is relevant to the discussion, the position of the first double bond from the methyl terminus is indicated by "n-x", where × is the first

double-bonded carbon atom counting from the methyl terminal end of the chain. Unlabeled fatty acid standards were purchased from Nu-Check Prep (Elysian, MN). Palmitic acid-d_4 (16:0-d_4) was purchased from Cambridge Isotope Laboratories (Tewksbury, MA). Arachidonic acid-d_8 (20:4-n6-d_8) and linoleic acid-d_4 (18:2-n6-d_4) were purchased from Cayman Chemicals (Ann Arbor, MI). Mouse monoclonal antibodies to hypoxia inducible factor (HIF) 1α (ab16066), HIF2α (ab157249), β-Actin (ab8226), and HRP conjugated Goat polyclonal to mouse IgG (ab97023) were purchased from Abcam (Cambridge, MA). All solvents used for LC-MS analysis were LC-MS grade and were purchased from Fisher Scientific (Waltham, MA).

Cell Culture

All cells except primary neurons were plated on a six well cell culture plate (CELLSTAR, Greiner Bio-One, Monroe, NC) at a density of 1.5 million cells per well three days before the experiment and maintained at 5% CO_2 at 37°C in DMEM/F-12 with 10% FBS and 5% Horse Serum. For experiments with primary cortical neurons, cells were seeded on a six well poly-d-lysine coated plate (Becton Dickinson, Franklin Lakes, NJ) at a density of 1 million cells per well and maintained at 5% CO_2 at 37°C in neurobasal medium containing 2 % B-27 Supplement (Life Technologies) and 0.5 mM Glutamax (Life Technologies). Half of the medium was replaced 24 hr after plating and every third day thereafter. Neurons were used for experiments after 10 days in culture.

Cell Counts and Cytotoxicity

To count cells, cells were trypsinized with 1mL 0.25% trypsin-EDTA (Gibco) for 10 min. The trypsin was inactivated by adding 1 mL DMEM/F12 with 10% FBS and 5% horse serum. The medium was triturated to wash cells off the plate, and the cell suspension was collected in a microfuge tube. A 100 μL aliquot was mixed with 10 μL trypan blue (0.4 % in PBS) and 10 μL was placed on a haemocytometer. Cells excluding trypan blue were counted in four fields of view and averaged to determine viable cells. The results were averaged across 3 cell culture wells.

Cytotoxicity was measured as a lactate dehydrogenase (LDH) percent release from cells (Korzeniewski & Callewaert 1983) using an enzymatic kit (BioVision, Milpitas, CA). Cytotoxicity was expressed as $(LDH_{medium}/LDH_{medium+cells})\times 100\%$.

Cell treatment with hypoxia and radioactive substrates

The growth medium was replaced with serum-free MEM and cells were incubated at 5% CO_2, 37°C, and 100% humidity in either 19% O_2 (normoxia) or 1% O_2 (hypoxia) 24 hours before treatment with lipogenic substrates. The medium used was not pre-equilibrated under 1% oxygen, however the incubation time under hypoxic conditions significantly exceeds the time required for oxygen removal from media that was estimated to be 2 h (Goldberg *et al.* 1986). The induction of hypoxia inducible factors HIF1α and HIF2α confirmed that cells were under hypoxic conditions (Fig 1, B and C). Hypoxic conditions were maintained using a Galaxy 48R incubator (Eppendorf, Hamburg, Germany) which controls oxygen levels by purging with nitrogen. After 24 h of preconditioning, the medium was replaced with either 2 mL serum-free MEM to determine total fatty acids in normoxic *versus* hypoxic cells by

mass spectrometry or 2 mL serum-free MEM containing a radiolabeled substrate to determine incorporation of specific substrates into lipids. Replacing the medium at 24 h ensures no nutrients were depleted during the preconditioning phase. The amounts of radiolabeled substrates used per cell culture well (2mL of medium) were: 2 μCi of [U-^{14}C]glucose (Glc, 3.5 μM in addition to 5.5 mM of unlabeled from MEM), 2 μCi [U-^{14}C]aspartate (Asp, 5 μM), 2 μCi [U-^{14}C]glutamine (Gln, 3.6 μM in addition to 2 mM of unlabeled from MEM), or 2 μCi [U-^{14}C]glutamate (Glu, 3.8 μM). The cells were treated with substrate under normoxic or hypoxic conditions for an additional 18 h. The medium was then removed and the cells were washed two times with ice cold PBS prior to lipid extraction.

Lipid Extraction

The cells were scraped into 0.5 mL methanol twice and transferred into a silanized (Sigmacote, Sigma Chemical Co., St. Louis, MO) screw top glass test tubes. For MS analysis, 100 ng of 16:0-d_4, 18:2n6-d_4, and 20:4n6-d_8, were added to the plates as internal standards before scraping. The lipids were extracted using the Folch procedure (Folch *et al.* 1957). Briefly, an additional 1 mL of methanol and 4 mL of chloroform were added to cells. The mixture was vortexed, sonicated, and centrifuged at 2000 *g* for 10 min. The supernatant was transferred into a new silanized screw top tube. The extract was washed once with 1.2 mL 0.9% NaCl and the upper phase was washed twice with 1.2 mL chloroform : methanol : water (3 : 48 : 47). The combined extract was dried under nitrogen and redissolved in 1 mL of hexane : 2-propanol (3 : 2) with vortexing. One hundred microliters was transferred into a 20 mL scintillation vial containing 10 mL Cytoscint™ (MP Biomedicals; Solon, OH) scintillation cocktail and counted in a scintillation counter (LS-6500, Beckman Coulter, Pasadena, CA). Another aliquot (450 μL) was subjected to saponification to release FA. Radiolabeled saponified samples were separated by thin layer chromatography (TLC) and analyzed for total FA radioactivity. Non-radiolabeled saponified samples were analyzed by UPLC-MS for total FA mass.

Saponification

Cell lipid extracts were transferred into screw-top test tubes, evaporated under nitrogen, re-dissolved in 180 μL methanol and 20 μL 5 M KOH in water, and saponified at 60°C for 60 min in a water bath. The solution was neutralized with the addition of 20 μL 5 M HCl followed by the addition of 780 μL 0.9% NaCl. The free fatty acids were extracted with 2 mL hexane 3 times. The hexane extracts were combined in a new silanized screw top tube. Saponification and extraction conditions were validated using [1,^{14}C] glycerol trioleate. The recovery of radio labeled free FA after separation by TLC was 94.8 ± 3.3 % (n=3).

Thin Layer Chromatography

To determine radioactivity in different lipid fractions including triacylglycerols (TAG), diacylglycerols (DAG), monoacylglycerols (MG), free FA, cholesterol (Ch), Cholesteryl esters (CE), and phospholipids (PL), the extracts were separated by TLC. The TLC plates (Partisil® LK6, Silica Gel, 60 Å, 250 μM, 20x20cm, Whatman, Maidstone, UK) were activated by heating to 110°C overnight. The sample was evaporated under nitrogen and re-

dissolved in 100 μL chloroform. Fifty microliters of the sample (22.5% from total lipid extract) was spotted on the plate. The plates were heated to 100°C for 5 min and placed in a TLC tank containing petroleum ether : diethylether : acetic acid (75 : 25 : 1.3 by volume) for 1hr (Marcheselli *et al.* 1988). The plates were visualized in iodine vapors. The bands corresponding to each lipid fraction were scraped and transferred into a scintillation vial with 1 mL methanol. Ten milliliters of Cytoscint™ scintillation cocktail was added and the samples were counted in a scintillation counter.

Fatty acid quantification with UPLC-MS Analysis

To prepare the saponified extracts for MS analysis, the extracts were evaporated under nitrogen and transferred to silanized microinserts (Agilent, Santa Clara CA; part #5181–8872) using two washes of 130 μl hexane. The samples in the microinserts were then evaporated under nitrogen and re-dissolved in 30 μl of acetonitrile : 2-propanol : water (1 : 1.28 : 1.28 by volume).

The LC system consisted of a Waters ACQUITY UPLC pump with a well-plate autosampler (Waters, Milford, MA) equipped with an ACUITY UPLC HSS T3 column (1.8 μM, 100 A pore diameter, 2.1×150 mm, Waters) and an ACUITY UPLC HSS T3 Vanguard precolumn (1.8 μM, 100 A pore diameter 2.1 × 5 mm, Waters). Two microliters of a sample was injected onto the column. The column temperature was 55°C and the autosampler temperature was 8°C.

The flow rate was 0.3 mL/min. Solvent A consisted of acetonitrile : water (40 : 60) with 10 μM ammonium acetate and 0.025% acetic acid. Solvent B was acetonitrile : 2-propanol (10 : 90) containing 10 μM ammonium acetate and 0.02% acetic acid. Solvent B was initially held at 40% for 0.1 min and was then increased to 99% over 10 min using a linear gradient. Solvent B was held at 99% for 8 min before returning to initial conditions over 0.5 min. The column was equilibrated for 2.5 min between injections.

Fatty acids were quantified using a quadrupole time-of-flight mass spectrometer (Q-TOF, Synapt G2-S, Waters) with electrospray ionization in negative ion mode as described previously (Brose *et al.* 2013). The cone voltage was 20 V and the capillary voltage was 1.51 kV. The source and desolvation temperatures were 110 °C and 350 °C respectively. The analyzer was operated with extended dynamic range at 10,000 resolution (fwhm at *m/z* 554) with an acquisition time of 0.1s. MS^E mode was used to collect data with the T-wave element alternated between a low energy of 2V and high energy states where the transfer T-wave element voltage was from 10–25 V (Bateman *et al.* 2002). The cone gas flow rate was 10 L/h and the desolvation gas flow was 1,000 L/h. Leucine enkephalin (400 pg/μl, ACN : water, 50 : 50 by volume) was infused at a rate of 10 μl/min for mass correction. MassLynx V4.1 software (Waters) was used for instrument control, acquisition, and sample analysis. Saturated FA were quantified against 16:0-d_4, mono- and di- unsaturated FA were quantified against 18:2-d_4, and polyunsaturated FA were quantified against 20:4n6-d_8 using a generated standard curve. Total FA was calculated as the sum of 6:0, 7:0, 8:0, 9:0, 10:0, 11:0, 12:0, 13:0, 14:0, 15:0, 16:0, 17:0, 18:0, 19:0, 20:0, 21:0, 22:0, 24:0, 16:1, 18:1, 20:1, 22:1, 24:1, 18:2, 20:2, 22:2, 18:3, 20:3, 22:3, 20:4, 20:4, 22:4, 22:5, 22:5, and 22:6.

Sodium dodecyl sulfate polyacrylamide gel electrophoresis (SDS-PAGE) and Western blot—Cells were lysed in RIPA buffer (20 mM Tris, pH 7.4, 150 mM NaCl, 1 mM Na_3VO_4, 10 mM NaF, 1 mM EDTA, 1 mM EGTA, 0.2 mM phenylmethylsulfonyl fluoride, 1 % Triton X-100, 0.1 % SDS, and 0.5% deoxycholate) with protease inhibitors (1 mM AEBSF, 0.8 μM Aprotinin, 21 μM Leupeptin, 36 μM Bestatin, 15 μM Pepstatin A, and 14 μM E-64, Sigma Chemical Co). Total protein concentration was measured using a dye binding assay with bovine serum albumin as a standard (Bradford 1976) using Bio-Rad Protein Assay (Bio-Rad, Hercules, Ca). The samples were diluted 1 : 1 with 2× Laemmli Sample Buffer (Bio-Rad) containing 5% β-Mercaptoethanol and heated to 95 °C for 5 min. Fifteen micrograms of protein was loaded onto a 10 % acrylamide gel (Mini-Protean TGX, Bio-rad) and separated for 40 min at 150 V using a running buffer consisting of 25 mM Tris, 192 mM Glycine, 0.1 % SDS; pH 8.3. The proteins were transferred to a polyvinylidene fluoride membrane (Pall Co.; Pensacola, Fl) by electroblotting at 300 mAmp for 1 h in transfer buffer (25 mM Tris, 192 mM Glycine, 12% MeOH). After transfer, the membrane was blocked with 3% BSA in TBS-T (50 mM Tris, 150 mM NaCl, 0.1 % Tween-20; pH 7.6) for 30 min at room temperature. The blocking solution was replaced with the primary antibody in TBS-T with 3% BSA and incubated overnight at 4 °C. The primary antibody solution was removed, rinsed for 10 min in TBS-T three times. The HRP conjugated secondary antibody was prepared in TBS-T containing 5% powdered milk. The membrane was incubated in the secondary antibody solution for 1.5 h followed by two 10 min TBS-T rinses. The membrane was visualized using the luminol based Amersham™ ECL™ Prime detection reagent (GE Healthcare, Buinghamshire, UK) and imaged using an Omega Lum G imager (Aplegen, Santa Barbara, CA). Optical density of the bands was quantified using VisionWorksLS 7 (UVP; Upland, CA) and normalized to actin.

Statistics

Statistical analysis was performed using GraphPad Prism 5 (GraphPad, San Diego; CA). Statistical comparisons were determined using a two-way, unpaired Student's *t* test or ANOVA with Tukey's post hoc test with statistical significance defined as <0.05. All values are expressed as mean ± SD. The sample size (n) represents independent measurements from (n) independent cell culture wells.

RESULTS

FA are increased in neuronal cells under hypoxia

FA levels are increased in various tissues under hypoxic conditions (Filipovic & Buddecke 1971, Yatsu & Moss 1971, Chabowski *et al.* 2006, Rankin *et al.* 2009, Boström *et al.* 2006), however the mechanisms for FA increase are still not completely understood. FA increase under hypoxia might be the result of decreased lipid oxidation or increased lipid biosynthesis (Whitmer *et al.* 1978, Filipovic & Buddecke 1971, Rankin et al. 2009, Boström et al. 2006). To address the contribution of biosynthesis to FA increase in neuronal cells, we first quantified total FA changes in the neuronal SH-SY5Y cell line (Fig. 1, A). Consistent with other model systems (Filipovic & Buddecke 1971, Yatsu & Moss 1971, Chabowski et al. 2006, Rankin et al. 2009, Boström et al. 2006), the neuronal total FA were significantly increased after 24 h and 42 h under hypoxia (1.2 and 1.3 fold, respectively, as compared to

the same incubation time under normoxia). The total FA mass increase was mainly accounted for by the increase in saturated and monounsaturated FA with carbon length from 14 to 24 (Table 1). Although shorter chain FA (10:0 and 12:0) were also significantly increased under hypoxia, the absolute mass for these FA was much lower compared to longer chain FA, decreasing their contribution to total FA increase.

Western blots were performed for HIF 1α and HIF 2α in order to confirm that cells were under hypoxia. (Fig 1, B and C). HIF 1α and HIF 2α were elevated 2.4- and 5.9- fold, respectively, at 1% oxygen compared to 19% oxygen indicating that the cells were responding to the hypoxia.

Incorporation of lipogenic substrates into FA under hypoxia in neuronal cell line

Next, we quantified the incorporation of different lipogenic substrates into lipids and FA in SH-SY5Y under hypoxic and normoxic conditions (Fig. 2). Because oxygen deprivation limits ATP production through oxidative phosphorylation under hypoxia, FA synthesis which requires ATP consumption for malonyl-CoA formation was expected to be decreased. Consistent with this assumption, glucose and aspartate incorporation into total lipids and FA was significantly decreased. Surprisingly, Gln and Glu incorporation into total lipids was significantly and dramatically increased 3.5- and 8.0- fold, respectively. Upon saponification of the [U-^{14}C]Glu labeled lipid extracts, 87.3% and 97.1% of radioactivity was recovered in the form of FA under normoxic and hypoxic conditions, respectively (Fig. 2, A and B), indicating that Glu was mainly used for acyl group synthesis in lipids.

Analysis of the radioactivity distribution between lipid classes indicates that synthesis of all lipid classes from Glu was proportionally increased under hypoxia except for TG which were increased to a higher extent, while Ch radioactivity was decreased (Fig. 3). The relative decrease in Ch synthesis resulted in a higher (97.1%) relative recovery of radioactivity in the form of FA upon saponification. The relative TG radioactivity increase upon hypoxia might be associated with increased deposition of newly synthesized FA in lipid droplets. In addition, the decrease of relative radioactivity in the non-acyl containing fraction Ch is consistent with predominant synthesis of FA with further esterification into acyl-containing lipids under hypoxia.

Interestingly, Glu was a preferred substrate for incorporation into FA compared to Gln as the incorporation rate for Glu was 10.0 fold higher as compared to Gln (Fig. 2). Because of the known excitatory and toxic effects of Glu on neuronal cells (Croce *et al.*, Choi *et al.* 1987, Olney & Sharpe 1969), we confirmed that the Glu concentration used (3.8 μM) was not toxic (Fig. 4, A), and did not affect the rate of incorporation of the other substrate Gln (Fig. 2, A and B). Glu concentration used (3.8 μM) was based on the specific activity of radiotracer L-[U-^{14}C] Glu, (260 mCi/mmol) to allow for a measurable incorporation of radiolabel into lipids. In addition, hypoxia did not affect the number of cells within the time of experiment for all cell types tested (42 h, Fig. 4, B), thus providing a rational to normalize the incorporation rates by the cell number. These data are consistent with primary neurons and astrocytes survival under hypoxia conditions with sufficiently supplied glucose (Goldberg et al. 1986, Haun *et al.* 1993, Haun *et al.* 1992).

Incorporation of lipogenic substrates into FA under hypoxia in primary cortical neurons

Because of the known differences in metabolism between cell lines and primary cell cultures (Sandberg & Ernberg 2005, Pan *et al.* 2009), we tested if primary cortical neurons also increase FA synthesis from Glu and Gln under hypoxia. Consistent with the cell line, primary neurons significantly increased lipid synthesis from Glu and Gln (3.0- and 2.0- fold, respectively, Fig. 5, A and B) under hypoxia, that was mainly (by 90.9%) accounted for by the increased FA synthesis (Fig. 6). Also consistent with neuronal cell line, the primary neurons preferred Glu *versus* Gln for FA synthesis (Fig. 5, A and B).

FA biosynthesis is specifically increased in neuronal cells

Next, we addressed the universal nature of the increased FA synthesis from Glu and Gln under hypoxia. Because the reductive decarboxylation of Glu is relatively increased under hypoxic conditions for FA synthesis as a universal mechanism for all cell lines previously tested (Leonardi et al. 2012, Metallo et al. 2012, Gameiro et al. 2013), we determined if FA synthesis from Gln/Glu is also increased in cell types other than neuronal cell lines and brain primary glial cells. Surprisingly, in non-neuronal cells analyzed Gln and Glu incorporation into FA under hypoxia was significantly reduced in BV2 (mouse microglial), PC12 (rat adrenal medulla pheochromocytoma), HepG2 (human liver hepatocellular carcinoma), and A549 (human lung alveolar adenocarcinoma) cell lines and primary rat cortical astrocytes, or was unchanged in A431 (human epidermoid carcinoma) and 786-O (human renal adenocarcinoma) (Fig. 5, A and B).

DISCUSSION

To address the mechanism for neuronal cells adaptation to hypoxia, we determined FA biosynthesis from different lipogenic substrates in neuronal and non-neuronal cell lines and primary cell cultures under hypoxia. Hypoxia dramatically and specifically induced FA synthesis from Gln/Glu in a neuronal cell line and primary neurons. In contrast, FA synthesis from Gln/Glu was decreased or unchanged in all non-neuronal cells tested under hypoxia. These results indicate that FA biosynthesis from Gln/Glu might be an adaptation pathway for neuronal cells to hypoxia.

The increase in both shorter and longer chain FA under hypoxia indicates that both de-novo synthesis and FA elongation are activated in neuronal cells. Although 8:0 and 10:0 were also increased, their contribution to total FA increase was lower because of the low relative mass in the cells (Table 1). However, this smaller pool of shorter chain FA is an intermediate pool in the de-novo FA synthesis. Together with a terminal product of de-novo synthesis (16:0) increase, these data further supports that de-novo FA synthesis is increased under hypoxia in neuronal cells. Interestingly, very long chain FA (22:0, 22:1, 24:4, and 24:1) which are produced through elongation and de-saturation pathways were also significantly increased under hypoxia. Because sphingolipids are known to be enriched in very long chain saturated and monounsaturated FA including 22:0, 22:1, 24:0, and 24:1 (Merrill 2011), this increase might indicate the formation of sphingolipids. Although the distribution of radioactivity in total PL was not changed under hypoxia (Fig. 3), this does not preclude the possibility that more sphingolipids were synthesized at the expense of glycerophospholipids. Importantly,

sphingolipids might modulate various intracellular pathways including pro- and anti-apoptotic signaling (Senkal *et al.* 2010, Thamiiselvan *et al.* 2002, Smyth *et al.* 1996), and further studies might be of interest to address FA incorporation into sphingolipids under hypoxia in neuronal cells.

Intriguingly, FA are known to be rapidly oxidized during uptake in brain tissue with more than 50% incorporation into brain aqueous phase (Golovko *et al.* 2005, Golovko & Murphy 2006), and ~75% of brain aqueous radioactivity is recovered in the form of Glu and Gln upon i.v. infusion of ^{14}C labeled 16:0 (Miller *et al.* 1987). In the present study we report, for the first time, an incorporation of Gln/Glu carbons back into FA. This might represent another type of carbon units recycling between lipids and neuromediators, and similar to FA β-oxidation/synthesis cycle, the shift of this cycle might be dictated by brain energy and/or neurotransmitter requirements.

A number of mechanisms might account for activation of FA biosynthesis under hypoxia including regulation of gene expression, phosphorylation, and allosteric regulation for rate limiting enzymes, and substrate availability. Activation under hypoxia may be controlled through the sterol regulatory element-binding proteins (SREBP) family. The likely candidate is SREBP-1 family, because it is known to activate transcription of genes mainly involved in FA, TG, and PL biosynthetic pathways including acetyl-CoA carboxylase (ACC), fatty acid synthase (FAS), and glycerol-3-phosphate acyltransferase (GPAT) (Pai *et al.* 1998, Horton *et al.* 2003). In contrast, activation of SREBP-2 mainly activates transcription of cholesterol biosynthesis genes (Pai et al. 1998, Horton et al. 2003). Importantly, FAS expression is increased under hypoxia (Tsui *et al.* 2013, Furuta *et al.* 2008), and hypoxia up-regulates the synthesis of SREBP-1, but not SREBP-2 (Li *et al.* 2007, Furuta et al. 2008). Putative involvement of SREBP-1 in this regulation is consistent with our finding that synthesis of all acyl-containing lipid classes, but not Ch was increased in neurons under hypoxia. Because SREBP is regulated differently in neurons and astrocytes (Pierrot *et al.* 2013), this provides a rational that increased FA synthesis from Gln/Glu in neurons, but not astrocytes, is up-regulated through SREBP-1 under hypoxia. In addition, FA synthesis is regulated through modulation of ACC activity, which is regulated by phosphorylation through the AMPK pathway (Munday 2002, Brownsey *et al.* 2006). Phosphorylation decreases its activity (Munday 2002, Brownsey et al. 2006), but Glu increases ACC activity by increasing phosphatase activity toward phosphorylated ACC (Baquet *et al.* 1993, Gaussin *et al.* 1996). In addition, ACC activity is enhanced by allosteric regulation by citrate and glutamate (Vagelos *et al.* 1963, Boone *et al.* 2000). Thus, our observed increase in neuronal FA synthesis is consistent with increased ACC activity via stimulation of phosphatase by Glu. In addition, under hypoxia aconitase expression may be increased (Tsui et al. 2013). The elevated expression of aconitase may increase conversion of isocitrate to citrate further stimulating increased ACC activity in neurons. However, hypoxia decreases uptake of Glu by astrocytes (Murugan *et al.* 2013, Boycott *et al.* 2007, Rao *et al.* 1990), and promotes Glu efflux from astroglia (Danbolt 2001, Malarkey & Parpura 2008, O'Shea 2002), thereby potentially reducing its allosteric regulation of ACC activity in astrocytes during hypoxia. Thus, hypoxia may account for both decreased Glu availability for FA synthesis and

decreased ACC activity in astrocytes, resulting in decreased FA synthesis in astrocytes observed in the present study.

The importance for FA biosynthesis from Gln/Glu under hypoxic conditions could be explained through different mechanisms. Because hypoxia did not affect the cell number in neuronal cell lines and primary cell cultures within the time frame of experiment, it is unlikely that increased FA synthesis is required for synthesis of membrane lipids to support cell proliferation as was speculated to explain increased lipogenesis in tumor cells (Porstmann *et al.* 2009). Alternatively, the FA synthesis might be required to balance Glu concentrations in neuronal tissue under hypoxia, thus protecting neurons from Glu induced excitotoxicity. It is well documented that Glu levels are dramatically (20- to 160- fold) increased in brain tissue upon ischemia (Hagberg *et al.* 1985, Takagi *et al.* 1993), and this increase might account for neuronal damage (Ankarcrona *et al.* 1995). This might also explain the higher levels of incorporation of Glu into FA compared to Gln which is not cytotoxic. However, astrocytes which are known to regulate Glu levels in the nervous system (McLennan 1976), decreased Glu utilization for FA synthesis under hypoxia. This might indicate that this is not a primary mechanism for Glu regulation in the whole nervous tissue, but rather a local mechanism associated with neurons under hypoxia. Although astrocytes actively uptake Glu from media and convert it to Gln, aspartate, and lactate depending upon exogenous Glu concentration under normoxic conditions (McKenna *et al.* 1996), hypoxia prevents uptake of Glu by astrocytes through downregulation of excitatory amino acid transporters (Murugan et al. 2013, Boycott et al. 2007, Rao et al. 1990), thus limiting astrocytic role in preventing Glu excitotoxicity under hypoxia. In line with this discussion, other studies demonstrated reverse the function of glutamate transporters under hypoxia that further facilitates astroglial Glu release (Danbolt 2001, Malarkey & Parpura 2008, O'Shea 2002). In addition to the decreased capacity of astrocytes to deplete extracellular Glu under hypoxia, the decreased Glu uptake in astrocytes might account for decreased Glu availability for FA synthesis that is consistent with decreased FA synthesis under hypoxia observed in the present study. Further studies are required to address the role of Glu transport in regulating substrate availability for FA synthesis in astroglia *versus* neurons under hypoxia.

In addition, our data indicate that Glu is a much preferred substrate for incorporation into FA than Gln under both normoxic and hypoxic conditions. This may indicate a substrate competition between Gln and Glu for reductive carboxylation which is known to be the major pathway for Gln utilization for lipogenic Acyl-CoA production (Leonardi et al. 2012, Metallo et al. 2012, Gameiro et al. 2013). To be utilized for FA synthesis, Gln first needs to be converted to Glu by glutaminase which is localized in the mitochondria (Roberg *et al.* 2010), thus adding an extra step for Gln utilization and defining Glu as a preferred substrate. In addition, the compartmentalization of Glu and Gln metabolism (McKenna *et al.* 2000, Zielke *et al.* 1998) will prevent mixing Glu and Gln product pools, thus each substrate might be channeled to FA synthesis through different enzymatic systems at different rates. If a free mixing of Glu and Gln metabolites occurs, than one would expect a significant dilution of radiolabeled products from Glu (3.8 μM) with unlabeled Gln (2mM). Because a similar concentration of radiolabeled Gln (3.6 μM) was used as alternative substrate, the same

specific activity of immediate precursor for FA synthesis (malonyl-CoA) would be expected for both substrates, and thus the same radioactivity of synthesized FA would be observed for both Glu and Gln in neuronal cells. Because the observed radioactivity of FA was much higher in the case of labeled Glu, these data support the earlier proposed compartmentalization for Glu and Gln metabolism (McKenna et al. 2000, Zielke et al. 1998). The assumption made in this discussion is that there is no preference for uptake of Glu *versus* Gln, and this assumption is consistent with the preferred Gln (but not Glu) utilization in neurons that is supplied by astrocytes (Zwingmann & Leibfritz 2003, McKenna et al. 2000).

Furthermore, increased FA biosynthesis in neuronal cells under hypoxia might be important for utilization of reduced cofactors ($NADH_2^+$, $NADPH_2^+$, $FADH_2$). One of the most important consequences of hypoxia is the decreased oxygen availability required for energy production through oxidative phosphorylation. As a result, ATP levels are decreased, while the reduced cofactors are significantly increased, limiting both energy and oxidative potential in cells. The tissue adapts to these conditions by switching to anaerobic glycolysis that yields 2 moles of ATP per mole of Glc. However, this pathway leads to further accumulation of reduced cofactors (2 moles of $NADH_2^+$). Because of the limited availability of oxidized cofactors in cells (NAD, NADP, FAD), it is essential to transfer hydrogen to other cellular acceptors to support anaerobic glycolysis and oxidative reactions. One of these acceptors is pyruvate (2 moles from one Glc), which are converted into lactate (2 moles per mole Glc) during anaerobic glycolysis. However, the high lactate levels (pK_a=3.86) produced from glucose (pK_a=12.28) rapidly decrease cellular pH, leading to neuronal death (Malisza *et al.* 1999, Payen *et al.* 1996). Thus, FA synthesis might be an alternative mechanism to utilize hydrogen and end-products of anaerobic glycolysis with much higher capacity and limited effect on pH as opposed to lactate accumulation. In fact, each mole of acetyl-CoA produced from 1 mole of Gln/Glu will utilize 2 moles of $NADH_2^+$ during incorporation into FA. In addition, reductive carboxylation which is the major pathway for Gln utilization for lipogenic Acyl-CoA production (Leonardi et al. 2012, Metallo et al. 2012, Gameiro et al. 2013) also consumes one reduced cofactor, further normalizing cellular reductive potential under hypoxia. It is reasonable to speculate that the amino group from Glu is used for pyruvate amination produced from glycolytic pathway, thus preventing pH drop. Alanine aminotransferase (ALAT; EC 2.6.1.2) that catalyzes amino group transfer between Glu and pyruvate is found in primary neurons and brain tissue (McKenna et al. 2000, Westergaard *et al.* 1993, Ruščák *et al.* 1982). However, the cytosolic pathway for FA synthesis requires malonyl-CoA production from acetyl-CoA which requires 1 mole of ATP per mole of malonyl-CoA. Thus, cytosolic FA biosynthesis will have a zero ATP balance when coupled to glycolysis. The mitochondrial FA synthesis is an alternative to the cytosolic pathway (Whereat & Rabinowitz 1975, Hiltunen *et al.* 2010, Hinsch *et al.* 1976, Seubert & Podack 1973, Hinsch & Seubert 1975, Podack & Seubert 1972). The free energy of the mitochondrial pathway is favorable for fatty acid biosynthesis without ATP consumption, and this pathway does not require malonyl-CoA and thus ATP for fatty acid biosynthesis (Hinsch et al. 1976, Seubert & Podack 1973, Hinsch & Seubert 1975, Podack & Seubert 1972), therefore leading to a positive ATP balance when linked to glycolysis.

Further studies are required to clarify if FA biosynthesis under hypoxia supports cellular reductive potential only, or energy charge, or both.

In summary, we demonstrated that FA biosynthesis from Glu and Gln is dramatically and specifically increased in neuronal cells and correlates with total FA increase under hypoxia. These results indicate that FA biosynthesis from Gln/Glu might be an adaptation pathway for neuronal cells survival under hypoxia.

Acknowledgments

We thank Ms. Svetlana Golovko for her excellent technical assistance. This publication was made possible by NIH Grant 1R01AG042819-01 (MYG), and NIH funded COBRE Mass Spec Core Facility Grant 1P30GM103329-01.

Abbreviations used

Asp	aspartate
DMEM/F-12	Dulbecco's Modified Eagle Medium/F-12
CE	cholesteryl esters
Ch	cholesterol
DAG	diacylglycerol
FA	fatty acids
Glc	glucose
Gln	Glutamine
Glu	glutamate
MG	monoacylglycerol
MS	mass spectrometry
PL	phospholipids
SDS-PAGE	sodium dodecyl sulfate polyacrylamide gel electrophoresis
TAG	Triacylglycerols
TLC	thin layer chromatography
UPLC	ultra-pressure liquid chromatography

REFERENCES

Ankarcrona M, Dypbukt JM, Bonfoco E, Zhivotovsky B, Orrenius S, Lipton SA, Nicotera P. Glutamate-induced neuronal death: A succession of necrosis or apoptosis depending on mitochondrial function. Neuron. 1995; 15:961–973. [PubMed: 7576644]

Baquet A, Gaussin V, Bollen M, Stalmans W, Hue L. Mechanism of activation of liver acetyl-CoA carboxylase by cell swelling. European Journal of Biochemistry. 1993; 217:1083–1089. [PubMed: 7901014]

Bateman RH, Carruthers R, Hoyes JB, Jones C, Langridge JI, Millar A, Vissers JPC. A novel precursor ion discovery method on a hybrid quadrupole orthogonal acceleration time-of-flight (Q-

TOF) mass spectrometer for studying protein phosphorylation. J Am Soc Mass Spectrom. 2002; 13:792–803. [PubMed: 12148804]

Boone AN, Chan A, Kulpa JE, Brownsey RW. Bimodal Activation of Acetyl-CoA Carboxylase by Glutamate. J. Biol. Chem. 2000; 275:10819–10825. [PubMed: 10753875]

Boström P, Magnusson B, Svensson P-A, Wiklund O, Borén J, Carlsson LMS, Ståhlman M, Olofsson S-O, Hultén LM. Hypoxia Converts Human Macrophages Into Triglyceride-Loaded Foam Cells. Arteriosclerosis, Thrombosis, and Vascular Biology. 2006; 26:1871–1876.

Boycott HE, Dallas M, Boyle JP, Pearson HA, Peers C. Hypoxia suppresses astrocyte glutamate transport independently of amyloid formation. Biochem. Biophys. Res. Commun. 2007; 364:100–104. [PubMed: 17927959]

Bradford M. A rapid and sensitive method for the quantitation of microgram quantities of protein utilizing the principle of protein-dye binding. Anal. Biochem. 1976; 72:248–254. [PubMed: 942051]

Brose S, Baker A, Golovko M. A Fast One-Step Extraction and UPLC–MS/MS Analysis for E2/D2 Series Prostaglandins and Isoprostanes. Lipids. 2013; 48:411–419. [PubMed: 23400687]

Brownsey RW, Boone AN, Elliott JE, Kulpa JE, Lee WM. Regulation of acetyl-CoA carboxylase. Biochemical Society Transactions. 2006; 34:223–227. [PubMed: 16545081]

Chabowski A, Górski J, Calles-Escandon J, Tandon NN, Bonen A. Hypoxiainduced fatty acid transporter translocation increases fatty acid transport and contributes to lipid accumulation in the heart. FEBS Letters. 2006; 580:3617–3623. [PubMed: 16753149]

Chen J-Q, Russo J. Dysregulation of glucose transport, glycolysis, TCA cycle and glutaminolysis by oncogenes and tumor suppressors in cancer cells. Biochimica et Biophysica Acta (BBA) - Reviews on Cancer. 2012; 1826:370–384.

Choi D, Maulucci-Gedde M, Kriegstein A. Glutamate neurotoxicity in cortical cell culture. The Journal of Neuroscience. 1987; 7:357–368. [PubMed: 2880937]

Clambey ET, McNamee EN, Westrich JA, et al. Hypoxia-inducible factor-1 alpha–dependent induction of FoxP3 drives regulatory T-cell abundance and function during inflammatory hypoxia of the mucosa. Proceedings of the National Academy of Sciences. 2012; 109:E2784–E2793.

Croce N, Bernardini S, Di Cecca S, Caltagirone C, Angelucci F. Hydrochloric acid alters the effect of l-glutamic acid on cell viability in human neuroblastoma cell cultures. Journal of Neuroscience Methods. 217:26–30. [PubMed: 23612442]

Danbolt NC. Glutamate uptake. Prog. Neurobiol. 2001; 65:1–105. [PubMed: 11369436]

DeBerardinis RJ, Mancuso A, Daikhin E, Nissim I, Yudkoff M, Wehrli S, Thompson CB. Beyond aerobic glycolysis: Transformed cells can engage in glutamine metabolism that exceeds the requirement for protein and nucleotide synthesis. Proceedings of the National Academy of Sciences. 2007; 104:19345–19350.

Filipovic I, Buddecke E. Increased Fatty Acid Synthesis of Arterial Tissue in Hypoxia. European Journal of Biochemistry. 1971; 20:587–592. [PubMed: 4325879]

Folch J, Lees M, Stanley GHS. A SIMPLE METHOD FOR THE ISOLATION AND PURIFICATION OF TOTAL LIPIDES FROM ANIMAL TISSUES. Journal of Biological Chemistry. 1957; 226:497–509. [PubMed: 13428781]

Furuta E, Pai SK, Zhan R, et al. Fatty Acid Synthase Gene Is Up-regulated by Hypoxia via Activation of Akt and Sterol Regulatory Element Binding Protein-1. Cancer Res. 2008; 68:1003–1011. [PubMed: 18281474]

Gallagher SA, Hackett PH. High-altitude illness. Emerg. Med. Clin. North Am. 2004; 22:329–355. [PubMed: 15163571]

Gameiro, Paulo A.; Yang, J.; Metelo, Ana M., et al. In Vivo HIF-Mediated Reductive Carboxylation Is Regulated by Citrate Levels and Sensitizes VHL-Deficient Cells to Glutamine Deprivation. Cell Metabolism. 2013; 17:372–385. [PubMed: 23473032]

Gaussin V, Hue L, Stalmans W, Bollen M. Activation of hepatic acetyl-CoA carboxylase by glutamate and Mg2+ is mediated by protein phosphatase-2A. Biochemical Journal. 1996; 316:217–224. [PubMed: 8645208]

Goldberg WJ, Kadingo RM, Barrett JN. Effects of ischemia-like conditions on cultured neurons: Protection by low Na +, low Ca 2+ solutions. J. Neurosci. 1986; 6:3144–3151. [PubMed: 3772425]

Golovko MY, Fargeman NJ, Cole NB, Castagnet PI, Nussbaum RL, Murphy EJ. à-Synuclein gene-deletion decreases brain palmitate uptake and alters the palmitate metabolism in the absence of à-synuclein palmitate binding. Biochemistry. 2005; 44:8251–8259. [PubMed: 15938614]

Golovko MY, Murphy EJ. Uptake and metabolism of plasma derived euricic acid by rat brain. J. Lipid Res. 2006; 47:1289–1297. [PubMed: 16525189]

Hagberg H, Lehmann A, Sandberg M, Nystrom B, Jacobson I, Hamberger A. Ischemia-Induced Shift of Inhibitory and Excitatory Amino Acids from Intra- to Extracellular Compartments. J. Cereb. Blood Flow Metab. 1985; 5:413–419. [PubMed: 4030918]

Hartman RE, Lee JM, Zipfel GJ, Wozniak DF. Characterizing learning deficits and hippocampal neuron loss following transient global cerebral ischemia in rats. Brain Res. 2005; 1043:48–56. [PubMed: 15862517]

Haun SE, Murphy EJ, Bates CM, Horrocks LA. Extracellular calcium is a mediator of astroglial injury during combined glucose-oxygen deprivation. Brain Res. 1992; 593:45–50. [PubMed: 1458319]

Haun, SE.; Murphy, EJ.; Bates, CM.; Horrocks, LA. Drugs in Development, Vol. 2: Ca 2+ Antagonists in CNS. Neva Press; Branford,CT: 1993. Nimodipine decreases astroglial injury during combined glucose-oxygen deprivation. In:; p. 299-306.

Hiltunen JK, Autio KJ, Schonauer MS, Kursu VAS, Dieckmann CL, Kastaniotis AJ. Mitochondrial fatty acid synthesis and respiration. Biochimica et Biophysica Acta (BBA) - Bioenergetics. 2010; 1797:1195–1202.

Hinsch W, Klages C, Seubert W. On the mechanism of malonyl CoA independent fatty acid synthesis. Different properties of the mitochondrial chain elongation and enoyl CoA reductase in various tissues. Eur. J. Biochem. 1976; 64:45–55. [PubMed: 1278159]

Hinsch W, Seubert W. On the Mechanism of Malonyl-CoA-Independent Fatty-Acid Synthesis. Eur. J. Biochem. 1975; 53:437–447. [PubMed: 237759]

Horton JD, Shah NA, Warrington JA, Anderson NN, Park SW, Brown MS, Goldstein JL. Combined analysis of oligonucleotide microarray data from transgenic and knockout mice identifies direct SREBP target genes. Proceedings of the National Academy of Sciences. 2003; 100:12027–12032.

Hota SK, Barhwal K, Singh SB, Ilavazhagan G. Chronic hypobaric hypoxia induced apoptosis in CA1 region of hippocampus: A possible role of NMDAR mediated p75NTR upregulation. Exp. Neurol. 2008; 212:5–13. [PubMed: 18466900]

Kirby BS, Crecelius AR, Voyles WF, Dinenno FA. Impaired Skeletal Muscle Blood Flow Control With Advancing Age in Humans: Attenuated ATP Release and Local Vasodilation During Erythrocyte Deoxygenation. Circ. Res. 2012; 111:220–230. [PubMed: 22647875]

Korzeniewski C, Callewaert DM. An enzyme-release assay for natural cytotoxicity. J. Immunol. Methods. 1983; 64:313–320. [PubMed: 6199426]

Leonardi R, Subramanian C, Jackowski S, Rock CO. Cancer-associated Isocitrate Dehydrogenase Mutations Inactivate NADPH-dependent Reductive Carboxylation. J. Biol. Chem. 2012; 287:14615–14620. [PubMed: 22442146]

Li J, Nanayakkara A, Jun J, Savransky V, Polotsky VY. Effect of deficiency in SREBP cleavage-activating protein on lipid metabolism during intermittent hypoxia. Physiological Genomics. 2007; 31:273–280. [PubMed: 17666524]

Lin C, Wu CJ, Wei IH, Tsai MH, Chang NW, Yang TT, Kuo YM. Chronic treadmill running protects hippocampal neurons from hypobaric hypoxia-induced apoptosis in rats. Neuroscience. 2013; 231:216–224. [PubMed: 23219906]

Maiti P, Singh SB, Muthuraju S, Veleri S, Ilavazhagan G. Hypobaric hypoxia damages the hippocampal pyramidal neurons in the rat brain. Brain Res. 2007; 1175:1–9. [PubMed: 17870061]

Malarkey EB, Parpura V. Mechanisms of glutamate release from astrocytes. Neurochem. Int. 2008; 52:142–154. [PubMed: 17669556]

Malisza KL, Kozlowski P, Ning G, Bascaramurty S, Tuor UI. Metabolite changes in neonatal rat brain during and after cerebral hypoxia-ischemia: a magnetic resonance spectroscopic imaging study†. NMR Biomed. 1999; 12:31–38. [PubMed: 10195327]

Marcheselli, VL.; Scott, BL.; Reddy, TS.; Bazan, NG.; Boulton, AA.; Baker, GB.; Horrocks, LA. Neuromethods 7 Lipids and Related Compounds. Clifton, NJ: Humana Press; 1988. Quantitative analysis of acyl group composition of brain phospholipids, neutral lipids, and free fatty acids; p. 83-110.

McKenna MC, Sonnewald U, Huang X, Stevenson J, Zielke HR. Exogenous Glutamate Concentration Regulates the Metabolic Fate of Glutamate in Astrocytes. J. Neurochem. 1996; 66:386–393. [PubMed: 8522979]

McKenna MC, Stevenson JH, Huang X, Hopkins IB. Differential distribution of the enzymes glutamate dehydrogenase and aspartate aminotransferase in cortical synaptic mitochondria contributes to metabolic compartmentation in cortical synaptic terminals. Neurochem. Int. 2000; 37:229–241. [PubMed: 10812208]

McLennan H. The autoradiographic localization of L-[3H]glutamate in rat brain tissue. Brain Research. 1976; 115:139–144. [PubMed: 974737]

Merrill AH. Sphingolipid and Glycosphingolipid Metabolic Pathways in the Era of Sphingolipidomics. Chem. Rev. 2011; 111:6387–6422. [PubMed: 21942574]

Metallo CM, Gameiro PA, Bell EL, et al. Reductive glutamine metabolism by IDH1 mediates lipogenesis under hypoxia. Nature. 2012; 481:380–384. [PubMed: 22101433]

Miller JC, Gnaedinger JM, Rapoport SI. Utilization of plasma fatty acid in rat brain: Distribution of [14 C]palmitate between oxidative and synthetic pathways. J. Neurochem. 1987; 49:1507–1514. [PubMed: 2889801]

Munday MR. Regulation of mammalian acetyl-CoA carboxylase. Biochemical Society Transactions. 2002; 30:1059–1064. [PubMed: 12440972]

Murugan M, Ling E-A, Kaur C. Dysregulated glutamate uptake by astrocytes causes oligodendroglia death in hypoxic perventricular white matter damage. Molecular and Cellular Neuroscience. 2013; 56:342–354. [PubMed: 23859823]

O'Shea RD. Roles and regulation of glutamate transporters in the central nervous system. Clin. Exp. Pharmacol. Physiol. 2002; 29:1018–1023. [PubMed: 12366395]

Olney JW, Sharpe LG. Brain lesions in an infant rhesus monkey treated with monosodium glutamate. Science. 1969; 166:386–388. [PubMed: 5812037]

Pai, J-t; Guryev, O.; Brown, MS.; Goldstein, JL. Differential Stimulation of Cholesterol and Unsaturated Fatty Acid Biosynthesis in Cells Expressing Individual Nuclear Sterol Regulatory Element-binding Proteins. J. Biol. Chem. 1998; 273:26138–26148. [PubMed: 9748295]

Pan C, Kumar C, Bohl S, Klingmueller U, Mann M. Comparative Proteomic Phenotyping of Cell Lines and Primary Cells to Assess Preservation of Cell Type-specific Functions. Molecular & Cellular Proteomics. 2009; 8:443–450. [PubMed: 18952599]

Pascual JM, Carceller F, Roda JM, Cerdán S. Glutamate, Glutamine, and GABA as Substrates for the Neuronal and Glial Compartments After Focal Cerebral Ischemia in Rats. Stroke. 1998; 29:1048–1057. [PubMed: 9596256]

Payen J-F, LeBars E, Wuyam B, Tropini B, Pepin J-L, Levy P, Decorps M. Lactate Accumulation During Moderate Hypoxic Hypoxia in Neocortical Rat Brain. J. Cereb. Blood Flow Metab. 1996; 16:1345–1352. [PubMed: 8898710]

Pierrot N, Tyteca D, D'Auria L, et al. Amyloid precursor protein controls cholesterol turnover needed for neuronal activity. EMBO Molecular Medicine. 2013; 5:608–625. [PubMed: 23554170]

Podack ER, Seubert W. On the mechanism of malonyl-CoA independent fatty acid synthesis. II. Isolation, properties and subcellular location of trans-2,3-hexenoyl-CoA and trans-2,3-decenoyl-CoA reductase. Biochimica et Biophysica Acta (BBA)/Lipids and Lipid Metabolism. 1972; 280:235–247.

Porstmann T, Santos CR, Lewis C, Griffiths B, Schulze A. A new player in the orchestra of cell growth: SREBP activity is regulated by mTORC1 and contributes to the regulation of cell and organ size. Biochem. Soc. Trans. 2009; 37:278–283. [PubMed: 19143646]

Rankin EB, Rha J, Selak MA, Unger TL, Keith B, Liu Q, Haase VH. Hypoxia-Inducible Factor 2 Regulates Hepatic Lipid Metabolism. Molecular and Cellular Biology. 2009; 29:4527–4538. [PubMed: 19528226]

Rao VL, Başkaya MK, Doğan A, Rothstein JD, Dempsey RJ. Traumatic brain injury down-regulates glial glutamate transporter (GLT-1 and GLAST) proteins in rat brain. J. Neurochem. 1990; 70:2020–2027. [PubMed: 9572288]

Raymond M, Li P, Mangin J-M, Huntsman M, Gallo V. Chronic Perinatal Hypoxia Reduces Glutamate–Aspartate Transporter Function in Astrocytes through the Janus Kinase/Signal Transducer and Activator of Transcription Pathway. The Journal of Neuroscience. 2011; 31:17864–17871. [PubMed: 22159101]

Roberg BÅ, Torgner IA, Kvamme E. Kinetics of a Novel Isoform of Phosphate Activated Glutaminase (PAG) in SH-SY5Y Neuroblastoma Cells. Neurochemical Research. 2010; 35:875–880. [PubMed: 19894115]

Ruščák M, Orlický J, Žúbor V, Hager H. Alanine Aminotransferase in Bovine Brain: Purification and Properties. J. Neurochem. 1982; 39:210–216. [PubMed: 7086411]

Sandberg R, Ernberg I. The molecular portrait of in vitro growth by meta-analysis of gene-expression profiles. Genome Biology. 2005; 6:R65. [PubMed: 16086847]

Schippers M-P, Ramirez O, Arana M, Pinedo-Bernal P, McClelland Grant B. Increase in Carbohydrate Utilization in High-Altitude Andean Mice. Curr. Biol. 2012; 22:2350–2354. [PubMed: 23219722]

Senkal CE, Ponnusamy S, Bielawski J, Hannun YA, Ogretmen B. Antiapoptotic roles of ceramide-synthase-6-generated C16-ceramide via selective regulation of the ATF6/CHOP arm of ER-stress-response pathways. The FASEB Journal. 2010; 24:296–308.

Seubert W, Podack ER. Mechanisms and physiological roles of fatty acid chain elongation in microsomes and mitochondria. MOLEC.CELL.BIOCHEM. 1973; 1:29–40. [PubMed: 4154399]

Smyth MJ, Perry DK, Zhang J, Poirier GG, Hannun YA, Obeid LM. prICE: a downstream target for ceramide-induced apoptosis and for the inhibitory action of Bcl-2. Biochem. J. 1996; 316:25–28. [PubMed: 8645213]

Takagi K, Ginsberg MD, Globus MYT, Dietrich WD, Martinez E, Kraydieh S, Busto R. Changes in Amino Acid Neurotransmitters and Cerebral Blood Flow in the Ischemic Penumbral Region Following Middle Cerebral Artery Occlusion in the Rat: Correlation with Histopathology. J. Cereb. Blood Flow Metab. 1993; 13:575–585. [PubMed: 8100237]

Thamiiselvan V, Li W, Sumpio BE, Basson MD. Sphingosine-1-phosphate stimulates human Caco-2 intestinal epithelial proliferation via p38 activation and activates ERK by an independent mechanism. In Vitro Cellular and Developmental Biology - Animal. 2002; 38:246–253. [PubMed: 12197778]

Tsui K-H, Chung L-C, Wang S-W, Feng T-H, Chang P-L, Juang H-H. Hypoxia upregulates the gene expression of mitochondrial aconitase in prostate carcinoma cells. Journal of Molecular Endocrinology. 2013; 51:131–141. [PubMed: 23709747]

Vagelos PR, Alberts AW, Martin DB. Studies on the Mechanism of Activation of Acetyl Coenzyme A Carboxylase by Citrate. Journal of Biological Chemistry. 1963; 238:533–540. [PubMed: 13995702]

Westergaard N, Varming T, Peng L, Sonnewald U, Hertz L, Schousboe A. Uptake, release and metabolism of alaume in neurons and astrocytes in primary cultures. J. Neurosci. Res. 1993; 35:540–545. [PubMed: 8377225]

Whereat AF, Rabinowitz JL. Aortic mitochondrial synthesis of lipid and its response to cholesterol feeding. Am. J. Cardiol. 1975; 35:567–571. [PubMed: 164112]

Whitmer JT, Idell-Wenger JA, Rovetto MJ, Neely JR. Control of fatty acid metabolism in ischemic and hypoxic hearts. Journal of Biological Chemistry. 1978; 253:4305–4309. [PubMed: 659417]

Wilson MH, Newman S, Imray CH. The cerebral effects of ascent to high altitudes. The Lancet Neurology. 2009; 8:175–191.

Yatsu FM, Moss SA. Brain Lipid Changes Following Hypoxia. Stroke. 1971; 2:587–593. [PubMed: 4367374]

Zielke HR, Collins RM, Baab PJ, Huang Y, Zielke CL, Tildon JT. Compartmentation of [14C]Glutamate and [14C]Glutamine Oxidative Metabolism in the Rat Hippocampus as Determined by Microdialysis. J. Neurochem. 1998; 71:1315–1320. [PubMed: 9721758]

Zwingmann C, Leibfritz D. Regulation of glial metabolism studied by 13C-NMR. NMR Biomed. 2003; 16:370–399. [PubMed: 14679501]

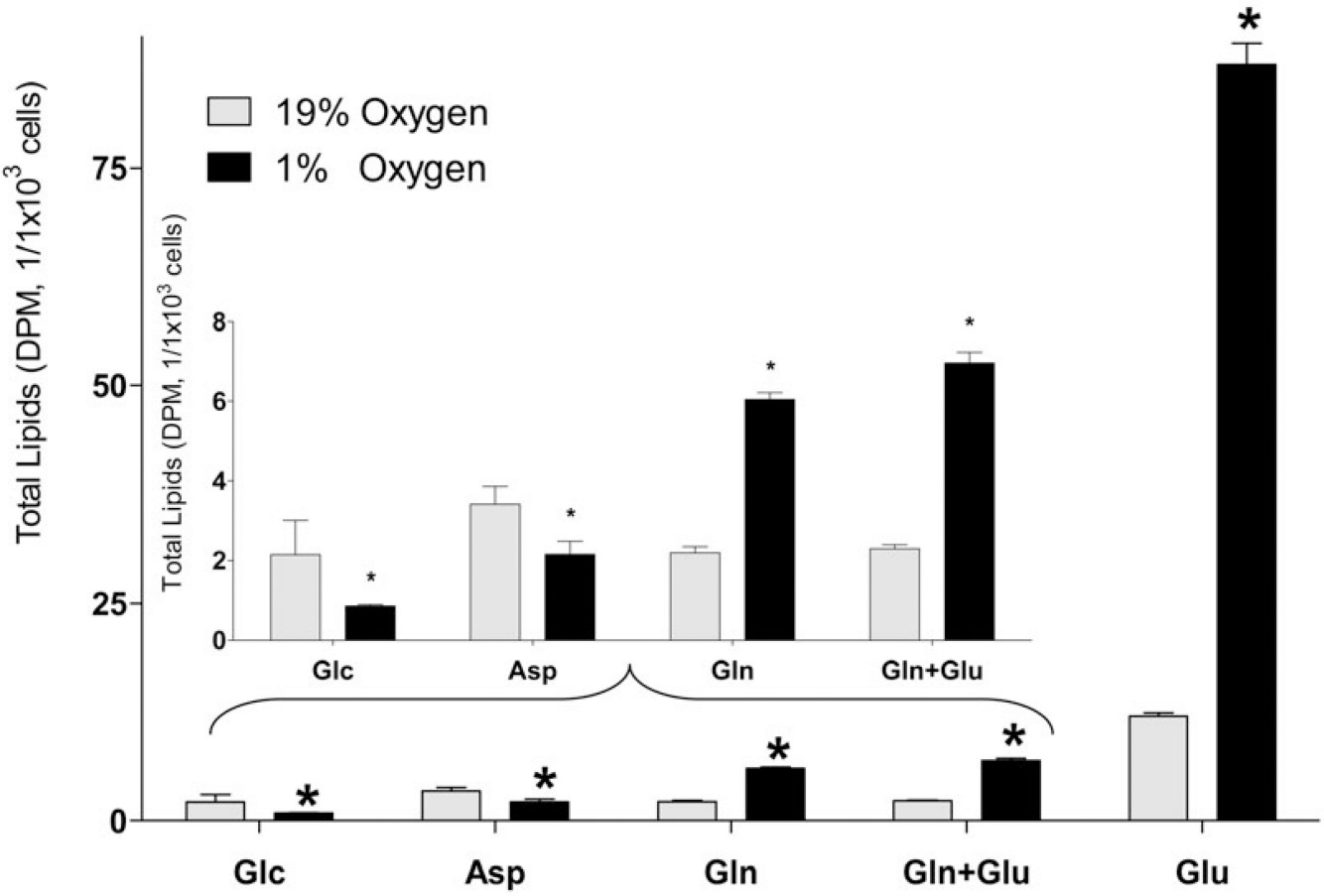

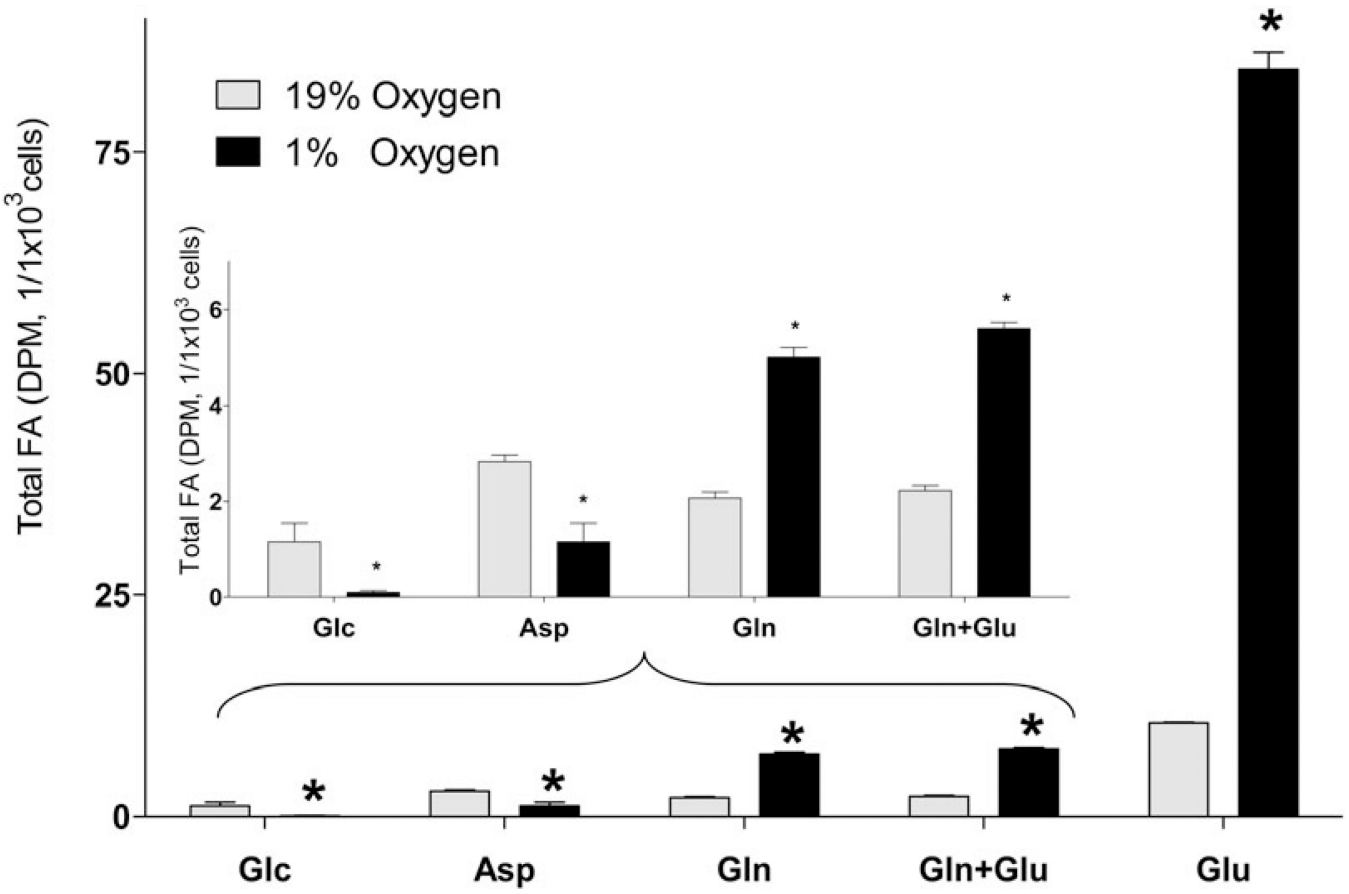

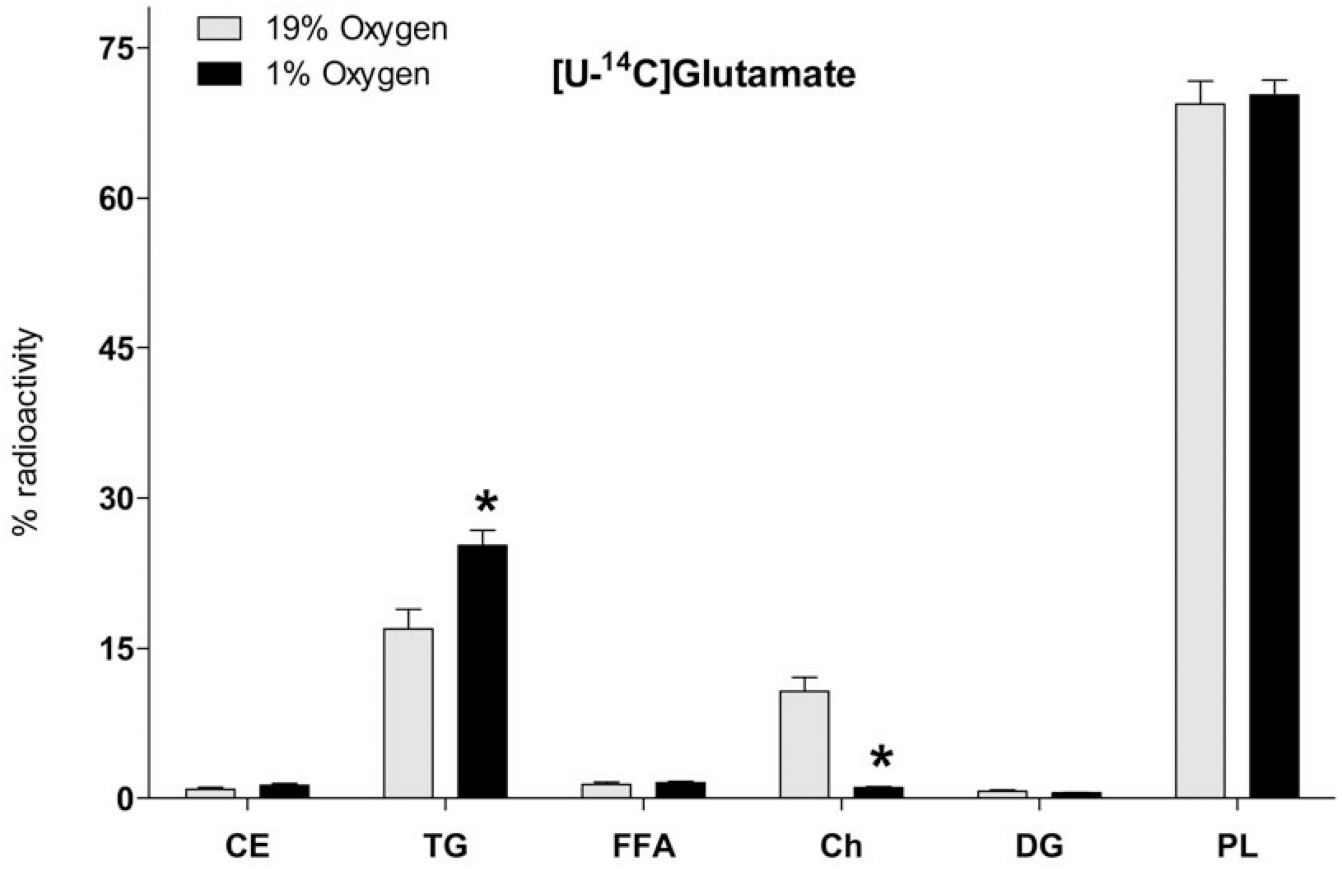

Fig. 1. Total fatty acid mass increase under hypoxic conditions in neuronal cell line

SH-SY5Y cells were incubated in serum-free MEM medium under normoxic (19% O_2) or hypoxic (1% O_2) conditions. Medium was changed for fresh serum-free medium after the first 24 h of incubation. **A**: Lipids were extracted from cells after 24 and 42 h of incubation using chloroform/methanol by the Folch protocol, saponified with KOH, and fatty acids extracted with hexane were analyzed using the UPLC-MS method as described in the Methods section. a – statistically different as compared to 0h; b – statistically different as compared to 19% O_2 at 24h; c – statistically different as compared to 19% O_2 at 42h using ANOVA with Tukey's post-test. Values are mean ± SD, n=6. **B**: A Western blot analysis of SH-SY5Y cell lysate at 42 h as described in the Methods section to confirm cell response to hypoxic conditions. **C**: Quantification of optical densities of the Western blots. * – statistically different as compared to 19% O_2 using Student's *t* test. Values are mean ± SD, n = 3.

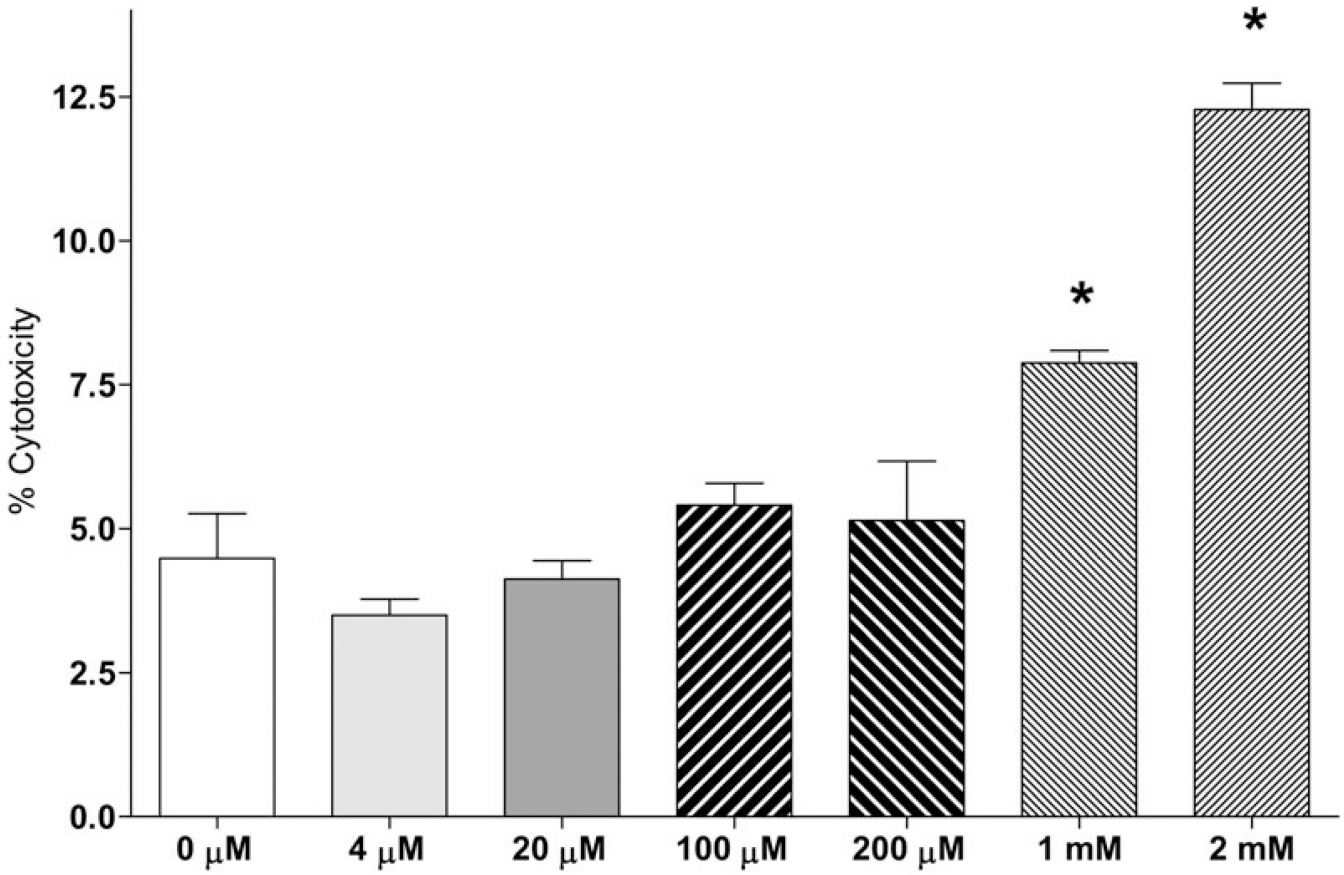

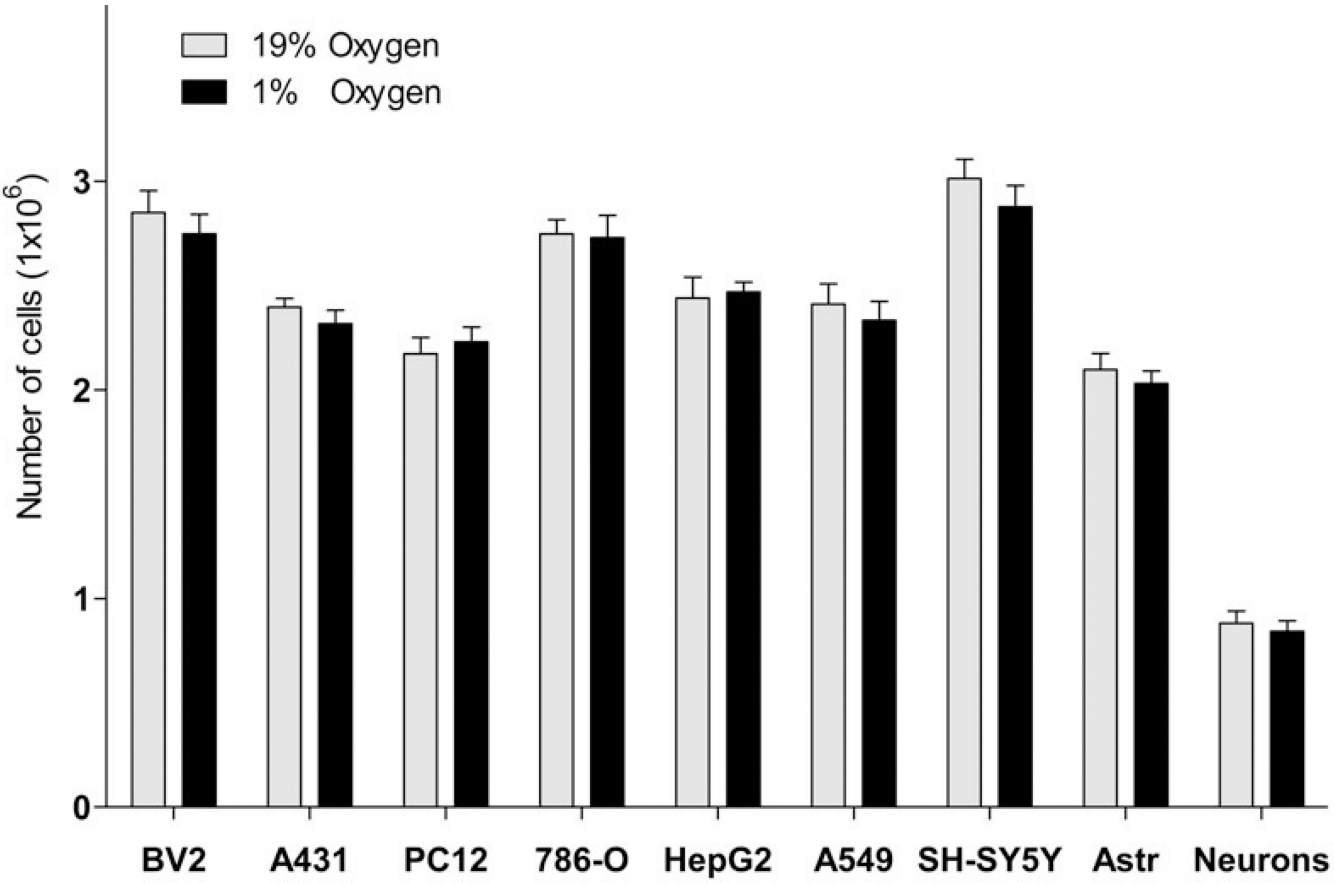

Fig. 2. Incorporation of radiolabeled substrates into total lipids and total fatty acids in a neuronal cell line

Incorporation of radiolabeled substrates into total lipids (**A**) and total (free + esterified) fatty acids (**B**) upon incubation of SH-SY5Y cells with 2 μCi of [U-^{14}C]glucose (Glc), [U-^{14}C]aspartate (Asp), [U-^{14}C]glutamine without non-labeled glutamate (Gln), [U-^{14}C]glutamine with 3.8 μM non-labeled glutamate (Gln+Glu), or [U-^{14}C]glutamate (Glu) for 18h under 19% O_2 (normoxia) and 1% O_2 (hypoxia). Cells were preconditioned in serum-free medium for 24 h under normal or hypoxic condition, and for another 18 h with radiolabeled tracer. At the end of incubation, lipids were extracted from cells using chloroform/methanol by the Folch protocol. An aliquot of the extract was analyzed for total lipid radioactivity (**A**). Another aliquot of the lipid extracts was saponified with KOH and separated by TLC for total fatty acid radioactivity analysis (**B**). Insets represent Glc, Asp, Gln, and Gln + Glu incorporation at a smaller scale. Addition of non-labeled aspartate (0.5 mM) did not affect the ^{14}C incorporation rates from all substrates. ***** - significantly different as compared to 19% O_2. Values are mean ± SD, n=3.

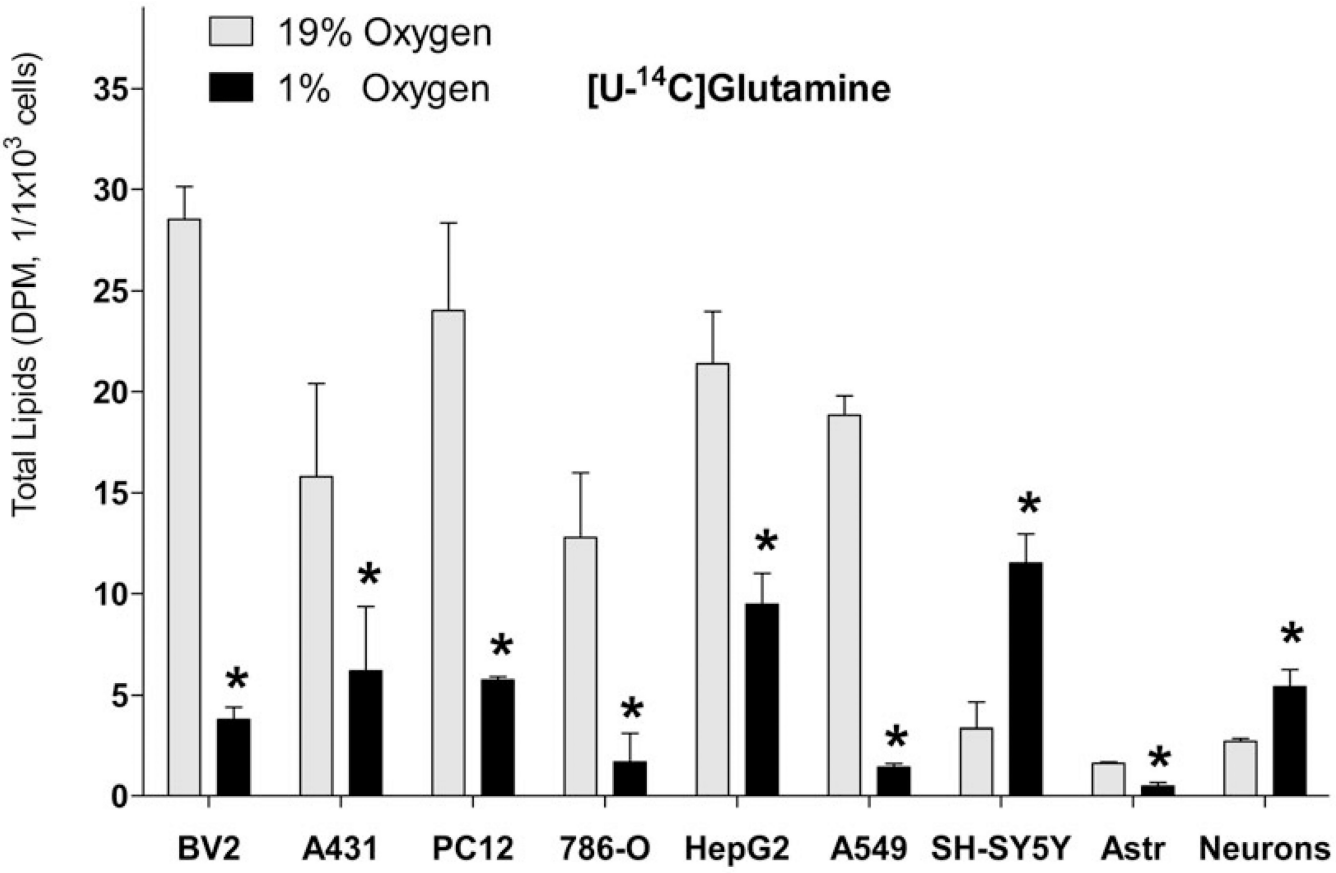

Fig. 3. Incorporation of glutamate radioactivity into lipid classes upon hypoxia in neuronal cell line

SH-SY5Y cells were preconditioned in serum-free MEM medium under normoxic (19% O_2) or hypoxic (1% O_2) conditions for 24 h, and for another 18 h with 2 μCi of [U-^{14}C]glutamate. Lipids were extracted from cells after 42 h of incubation using chloroform/methanol by the Folch protocol, separated by TLC and radioactivity of individual lipid classes was analyzed by liquid scintillation counting. Abbreviations are: CE, cholesteryl esters; TG, TAGs; FFA, free fatty acids; DAG, diacylglycerols; Ch, cholesterol; PL, phospholipids; * - significantly different as compared to 19% O_2. Values are mean ± SD, n = 3.

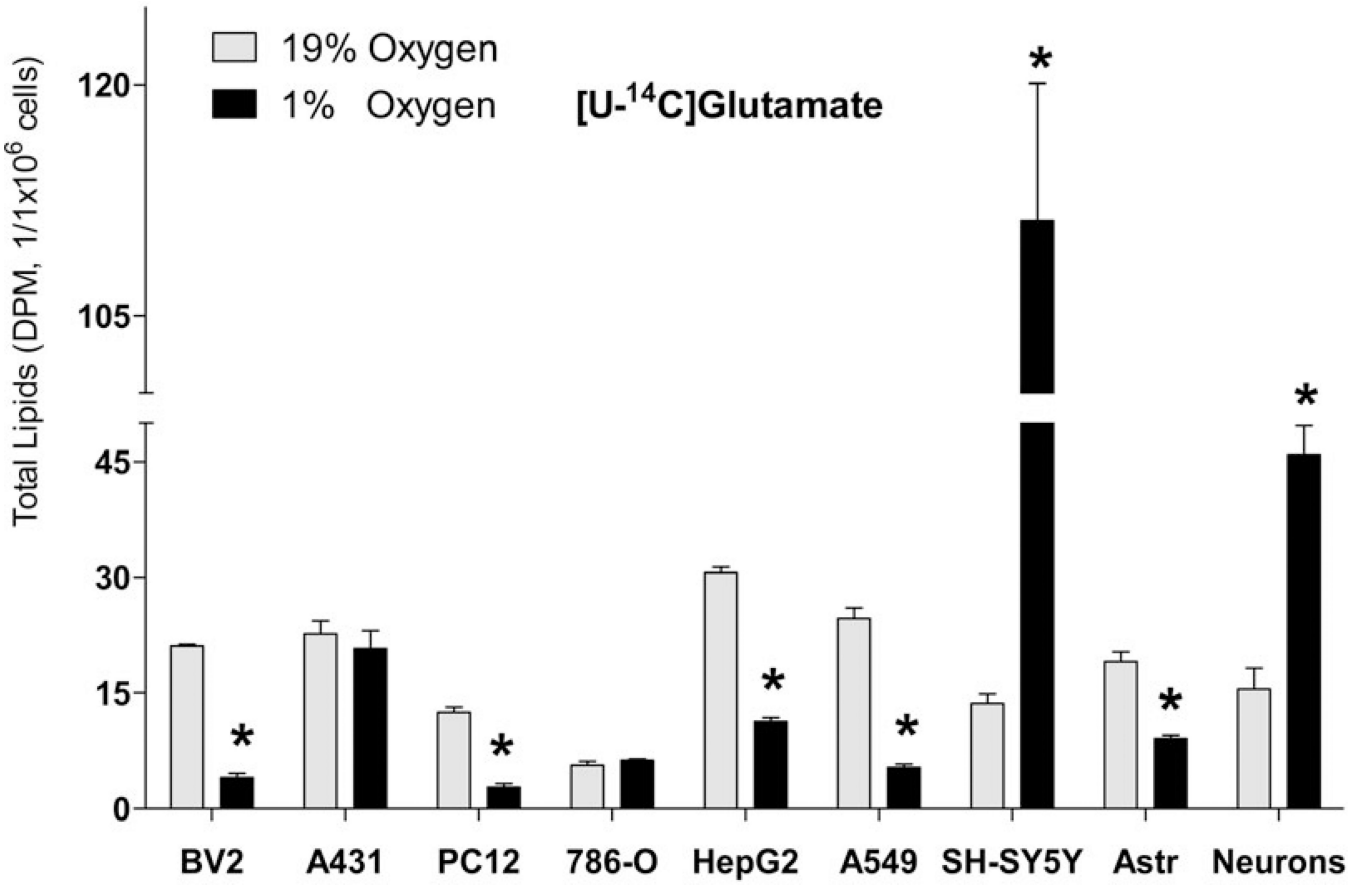

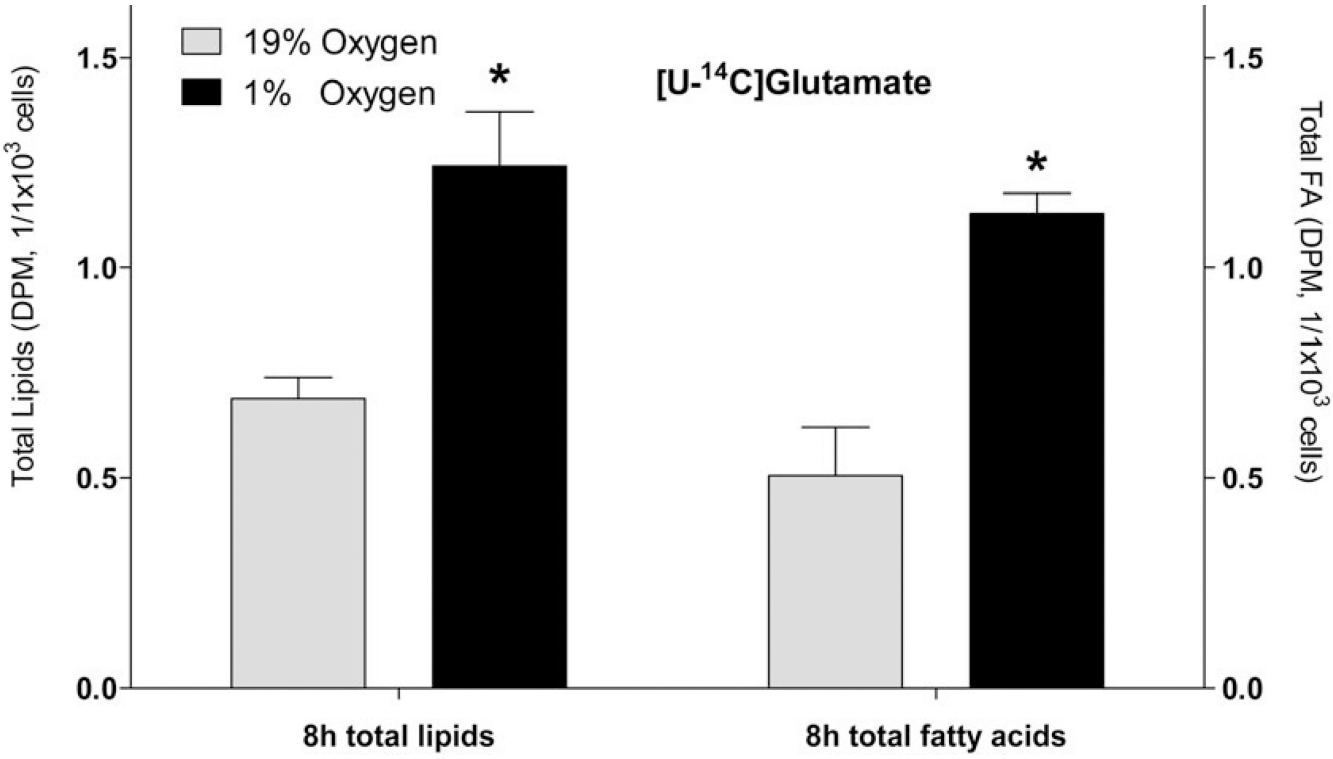

Fig. 4. Glutamate cytotoxicity and effect of hypoxia on the number of cells

Cytotoxic effect of glutamine substitution with glutamate in a neuronal cell line (**A**) and the effect of hypoxia on number of cells (**B**). **A**: SH-SY5Y cells were incubated in MEM medium (5.5 mM glucose and 2 mM glutamine) for 72 h, for another 24 h in serum-free MEM, and then for 18 h in MEM containing an indicated concentration of glutamate. Glutamine concentration was decreased by the indicated amount of glutamate added. Cytotoxicity was measured by LDH percent release. ***** - significantly different as compared to control (0 μM glutamate). Data are mean ± SD, n=6. **B**: BV2 (mouse microglial cell line), A431 (human epidermoid carcinoma cell line), PC12 (rat adrenal medulla pheochromocytoma cell line), 786-O (human renal adenocarcinoma cell line), HepG2 (human liver hepatocellular carcinoma cell line), A549 (human lung alveolar adenocarcinoma cell line), SH-SY5Y (human neuron-like neuroblastoma cell line), rat cortical astrocytes (Astr), or rat primary cortical neurons were incubated in serum-free medium under normoxic or hypoxic condition. After 24h of incubation, medium was changed for a fresh serum-free medium and cells were incubated for another 18 h under the same conditions. The cells were counted at the end of incubation. Data are mean ± SD, n=3.

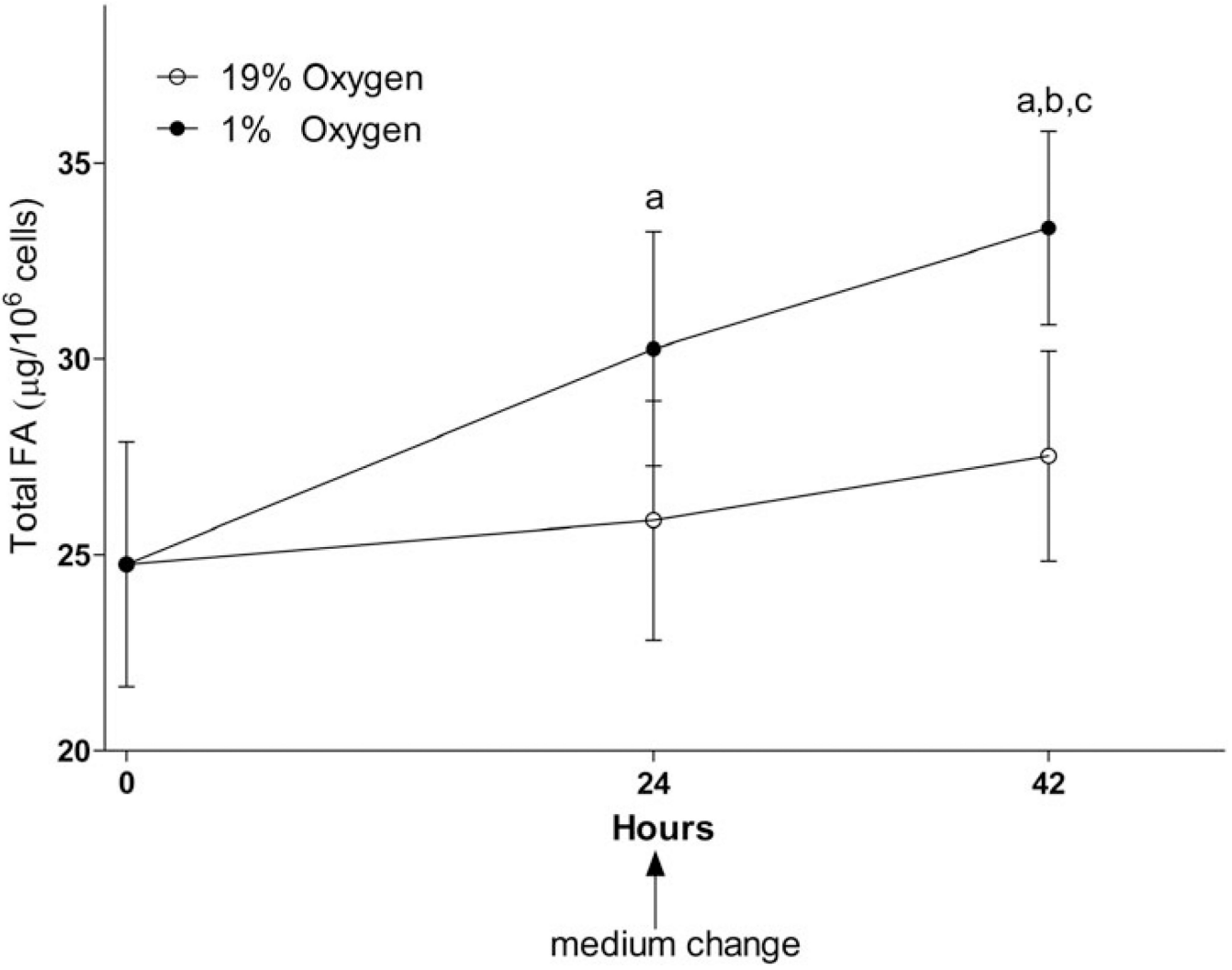

Fig. 5. Incorporation of radiolabeled glutamine and glutamate into lipids in cell lines and primary cell cultures

Incorporation of radiolabeled [U-^{14}C]glutamine (2 μCi of, **A**) and [U-^{14}C]glutamate (2 μCi of, **B**) into total lipids under 19% O_2 (normoxia) and 1% O_2 (hypoxia). Cells were preconditioned in serum-free medium for 24 h under normoxic or hypoxic conditions, and for another 18 h with radiolabeled tracer. At the end of incubation, lipids were extracted from cells using chloroform/methanol by the Folch protocol and analyzed for radioactivity. ***** - significantly different as compared to 19% O_2. Values are mean ± SD, n=3.

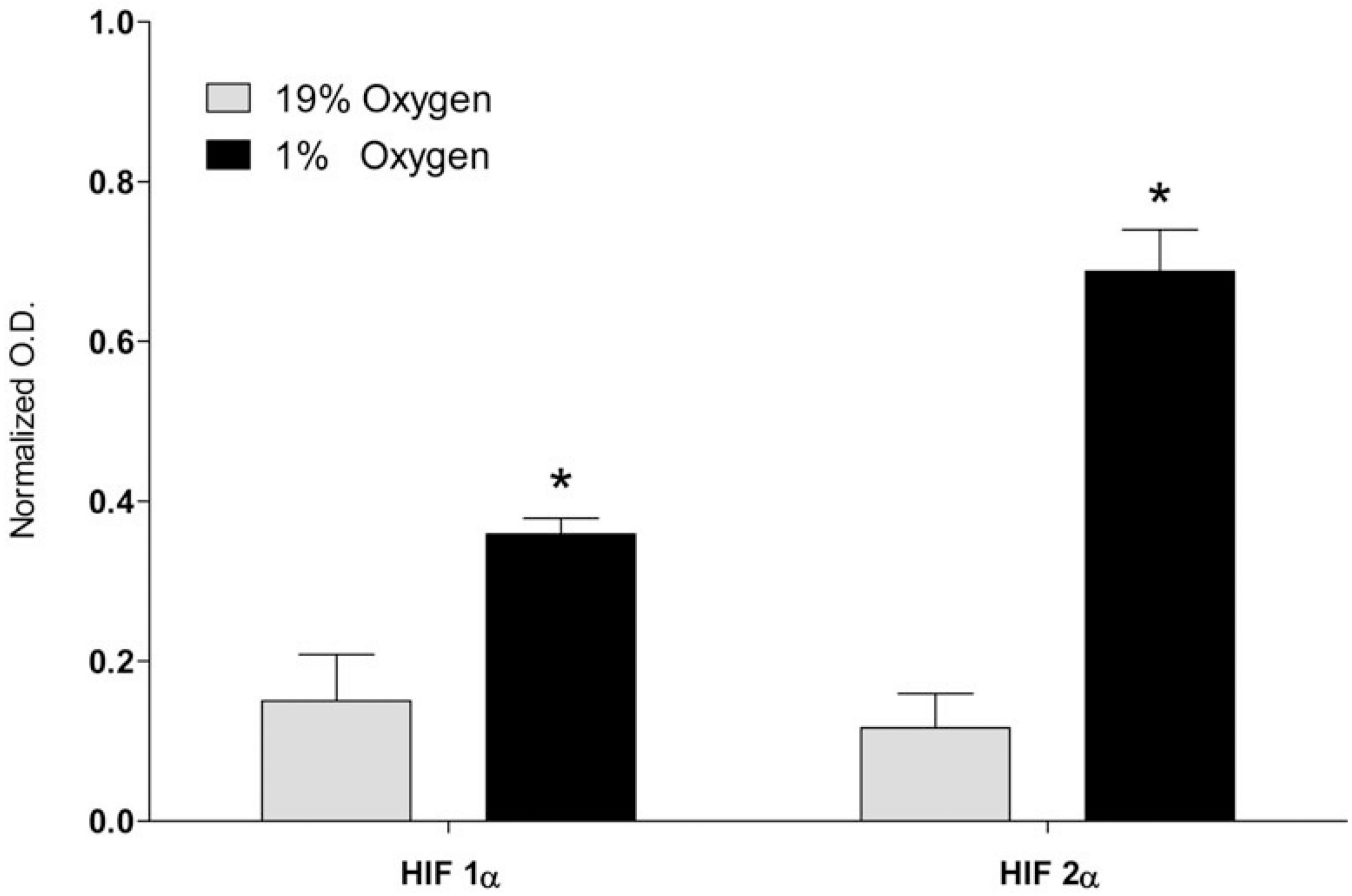

Fig. 6. The effect of hypoxia on incorporation of radiolabeled glutamate into total lipids and total fatty acids in primary rat cortical neurons

Primary rat cortical neurons were preconditioned in serum-free medium for 24 h under normal (19% O_2) and hypoxic condition (1% O_2) or, and for another 8 h with radiolabeled [U-^{14}C] glutamate (2 μCi). At the end of incubation, lipids were extracted from cells using chloroform/methanol by the Folch protocol and analyzed for radioactivity. An aliquot of lipid extract was saponified with KOH and separated on TLC for fatty acid analysis. ***** - significantly different as compared to 19% O_2. Values are mean ± SD, n=3.

Table 1

Effect of hypoxia on total fatty acid composition in neuronal cell line

SH-SY5Y cells were incubated in serum-free MEM medium under normoxic (19% O_2) or hypoxic (1% O_2) conditions. Medium was changed for fresh serum-free medium after the first 24 h of incubation. Lipids were extracted from cells after 24 and 42 h of incubation using chloroform/methanol by the Folch protocol, saponified with KOH, and fatty acids extracted with hexane were analyzed using the UPLC-MS method as described in the Methods section.

	0h		19% O_2, 24h, ng/10^6cells		1% O_2, 24h, ng/10^6cells			19% O_2, 42h, ng/10^6cells		1% O_2, 42h, ng/10^6cells		
	AV	SD	AV	SD	AV	SD	Statistics	AV	SD	AV	SD	Statistics
6:0	N/D		N/D		N/D			N/D		N/D		
7:0	0.23	0.25	0.25	0.33	0.21	0.18	ns	0.18	0.04	0.19	0.06	ns
8:0	N/D		N/D		N/D		ns	N/D		N/D		ns
9:0	0.14	0.07	0.13	0.08	0.14	0.07	ns	0.07	0.02	0.12	0.06	ns
10:0	0.89	0.55	0.88	0.25	1.69	0.52	*a,b,c*	0.67	0.18	1.78	0.58	*a,b,c*
11:0	0.87	0.20	0.72	0.33	0.85	0.31	ns	0.51	0.13	0.85	0.22	ns
12:0	22.84	4.56	19.24	5.03	32.03	9.62	*b,c*	19.42	4.14	41.35	10.74	*a,b,c*
13:0	4.85	0.75	4.65	1.98	4.37	0.94	ns	3.28	0.86	4.74	1.08	ns
14:0	726.45	100.19	798.51	250.11	1052.91	284.69	ns	829.03	175.57	1427.00	304.47	*a,b,c*
15:0	44.26	6.18	44.64	11.18	44.45	5.91	ns	36.78	9.15	46.28	5.59	ns
16:0	3370.64	336.82	3562.39	634.44	4063.41	587.06	ns	3690.03	465.92	4597.37	564.21	*a,b,c*
16:1	945.35	138.51	1011.93	271.58	993.67	157.85	ns	1220.82	208.38	1020.03	131.19	ns
17:0	139.41	17.52	126.53	27.37	141.92	20.00	ns	109.94	17.92	144.22	16.62	ns
18:0	4328.85	386.87	4819.38	1230.07	5936.25	990.68	*a*	5400.10	1065.68	6640.07	812.39	*a,b*
18:1	3962.09	470.67	3904.95	942.57	4284.25	554.36	ns	4551.58	612.88	4614.13	316.45	ns
18:2	511.35	63.04	519.29	131.86	598.00	101.56	ns	580.76	106.54	589.03	62.15	ns

	0h		19% O_2, 24h, ng/10^6cells		1% O_2, 24h, ng/10^6cells			19% O_2, 42h, ng/10^6cells		1% O_2, 42h, ng/10^6cells		
	AV	**SD**	**AV**	**SD**	**AV**	**SD**	**Statistics**	**AV**	**SD**	**AV**	**SD**	**Statistics**
18:3	50.63	6.82	48.32	13.38	53.36	10.31	ns	56.02	11.23	50.61	5.58	ns
19:0	43.89	6.18	43.16	11.68	55.25	12.29	ns	43.96	9.81	59.30	9.59	ns
20:0	152.25	35.82	159.03	44.69	431.10	124.51	*a,b,c*	149.22	25.90	522.95	110.17	*a,b,c*
20:1	693.88	96.03	746.22	237.68	1044.91	239.60	*a*	815.16	146.66	1162.67	167.62	*a,b,c*
20:2	532.90	66.22	571.78	176.38	707.58	149.18	ns	571.78	176.38	754.56	109.46	ns
20:3	949.30	79.45	1002.38	260.87	966.34	180.84	ns	1126.15	173.89	1063.66	159.00	ns
20:4	2645.70	276.90	2630.87	608.06	2863.69	451.02	ns	2507.27	423.77	2995.57	290.15	ns
21:0	8.21	2.22	7.43	3.59	7.87	1.70	ns	4.21	0.83	7.80	1.21	ns
22:0	37.38	10.76	37.89	8.09	131.97	31.76	*a,b,c*	29.74	4.00	158.37	27.04	*a,b,c*
22:1	122.68	12.67	130.66	53.86	340.97	98.94	*a,b,c*	145.04	29.69	379.74	69.29	*a,b,c*
22:2	95.65	9.78	103.53	35.86	158.34	43.94	*a*	101.75	25.57	176.64	45.45	*a,b,c*
22:3	1346.71	101.66	1472.59	427.46	1416.27	302.78	ns	1506.08	292.17	1685.74	317.79	ns
22:4	1145.20	100.99	1156.08	207.11	1380.41	189.61	ns	1108.36	174.70	1338.77	96.58	ns
22:5	1216.77	119.75	1261.40	308.66	1366.06	221.57	ns	1348.31	273.17	1446.45	182.63	ns
22:6	1548.18	175.65	1580.04	449.88	1750.60	282.90	ns	1481.63	300.36	1891.23	205.01	ns
24:0	58.77	23.67	57.58	27.22	164.51	35.26	*a,b,c*	32.01	7.44	186.93	31.15	*a,b,c*
24:1	45.05	4.24	46.66	18.93	256.15	79.81	*a,b,c*	53.09	9.57	317.48	73.40	*a,b,c*
total	24751.35	3124.52	25869.07	3049.82	30249.51	2982.77	*a*	27522.96	2680.18	33325.66	2468.09	*a,b,c*

a – statistically different as compared to 0h;

b – statistically different as compared to 19% O_2 at 24h;

c – statistically different as compared to 19% O_2 at 42h;

ns – not statistically different from all conditions; N/D – below quantification limits.
Values are mean ± SD, n=6.